NTNU – Trondheim
Norwegian University of
Science and Technology

Lubrication Oil Flow Simulation in Connecting Rod

Ivar Audun Lothe Alendal

Master of Science in Mechanical Engineering
Submission date: July 2015
Supervisor: Kjell H. Holthe, KT
Co-supervisor: Eilif Pedersen, IMT

Norwegian University of Science and Technology
Department of Structural Engineering

Abstract

Lubrication oil-flow in the crank system of an medium size diesel engine running at 750 RPM was modeled and analyzed. The model was built up by combining models from several studies in both engine lubrication systems and pipe flow modal analysis. It is first used to analyze a system where the oil supply lines are fully open during the complete engine cycle. Results showed that these designs need a very high oil supply pressure to maintain a positive pressure in the connecting rod at all times. Having a positive pressure is important to prevent cavitation in the oil channels, and to ensure a continuous flow of cooling oil. Secondly the model was used to analyze a system where the big-end bearing tracks runs only half way around the circumference, closing the flow when the piston is in the lower region of the cycle. Such a design allowed for a lower oil supply pressure, as the channel closes when the oil is forced back. However, high amplitude pressure waves were introduced by the opening and closing procedure. By trimming design parameters and changing the valve-characteristics, it was possible to reduce the problem to a extent where it could not cause any problems. Various suggestions are discussed in controlling the extent of the pressure peaks.

Sammendrag

Oljetilførsel gjennom et hveivsystem i en medium størrelse diesel motor med turtall på 750 omdreininger per minutt ble modellert og analysert. Modellen ble basert på modeller bygget i tidsskrifter innen motorsmørningsystemer og modal analyse i hydraulikkrør. Modellen blir først brukt til å analysere en motor der oljekanalene er åpne gjennom hele motorens syklus. Resultater viste at et slikt design trenger et veldig høyt oljetrykk for å unngå problemer med kavitasjon som følge av undertrykk. Modellen ble også brukt til å analysere et system der oljelagrene i krank-lageret stenger oljetilførselen når stempelet er i nedre halvdel av syklus. Ved å bruke en slik konfigurasjon kunne en bruke et lavere trykk på oljetilførselen, men da oppstod store problemer med trykkbølger. Ved å justere parametre og endre i ventil-karakterestikken på ventilsystemet kunne man så og si eliminere disse problemene. I tillegg er det lagt fram noen forslag til hvordan man ytterligere kan kontrollere disse trykkvariasjonene.

Introduction

A reliable flow of oil through the crank system in a piston engine is important as it is used for both lubrication and cooling. The oil is delivered to the piston through the connecting rod and the crankshaft. Both these parts are subjected to high acceleration forces. Especially in the connecting rod, these forces together with the inertia of the oil can cause transient oilfow and pressure waves. It is of interest to know under what conditions the transients exists, and what parameters that influence the results. A general model is built for analyzing the transient oilflow in a medium sized diesel engine.

Contents

List of Figures

List of Tables

Abbreviations

RPM	**R**evolutions **P**er **M**inute - Engine rotational speed
TDC	**T**op **D**ead **C**entre - Piston is at the top of the bore
BDC	**B**ottom **D**ead **C**entre - Piston is at the bottom of the bore
Small-end	The part of the connecting rod where the piston attaches
Big-end	The part of the connecting rod where the crankshaft attaches
Stroke	Piston travel distance from TDC to BDC
Bore	Diameter of the bore and the piston
Con-rod	Connecting rod

Symbols

r_1	Main journal radius	m
L	Connecting rod length	m
L_{crc}	Connecting rod oil channel length	m
r_{crc}	Connecting rod oil channel radius	mm
α	Connecting rod angle	radians
$\dot{\alpha}$	Connecting rod angular speed	radians/sec^2
ax_r	Connecting rod axial acceleration	m/s^2
R	Crankshaft stroke radius	m
r_{csc}	Crankshaft rod channel radius	mm
L_{csc}	Crankshaft oil channel length	m
θ	Crankshaft angle	radians
ω	Crankshaft angular speed	radians/sec
y_p	Piston position	m
v_p	Piston velocity	m/s
a_p	Piston acceleration	m/s^2
c	Oil acoustic velocity	m/s
ν	Oil kinematic viscosity	Pas
ρ	Oil density	Kg/m^3
Re	Reynolds number	
P_{set}	Oil pump delivery pressure	Bar
R_f	Hagen-Poiseuille Friction coefficient	Pas/m^2
n	Engine speed	RPM
e	Bond-graph effort	Pa
f	Bond-graph flow	m^3/s
p	Bond-graph momentum	N/m^{2}s

q	Bond-graph displacement	m^3
R	Bond-graph resistance	
I	Bond-graph inertia	
C	Bond-graph capacitance	
Sf	Bond-graph set flow	
Se	Bond-graph set effort	
1	Bond-graph 1 junction	
0	Bond-graph junction	
TF	Bond-graph transformer junction	
GY	Bond-graph gyrator junction	

Chapter 1

Introduction

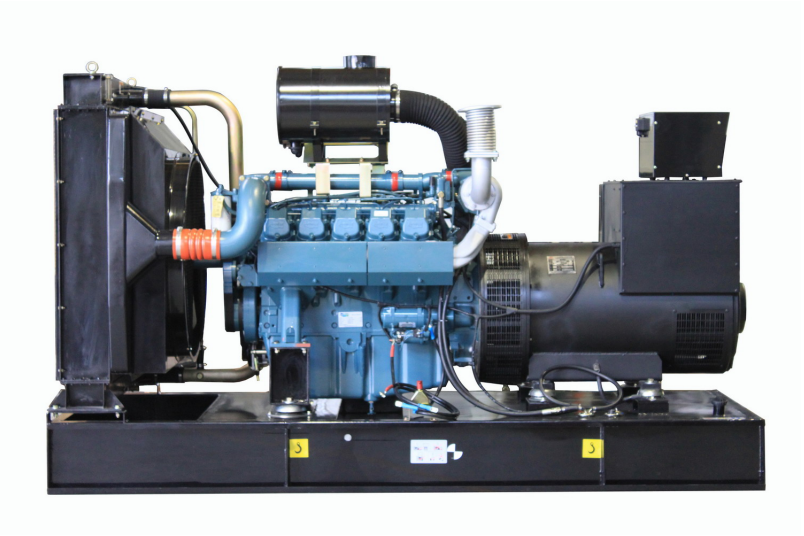

FIGURE 1.1: Doosan Daewoo Engine Diesel Generator

1.1 Background

Medium sized piston engines are used for power production in many industries. Typical installations range from second generators on ships, to hospital emergency generators. The reliability of these machines is very important, as they in some cases are expected to start from cold and then deliver electricity within seconds, running at full power. Reliable delivery of lubrication oil in motors are essential as it is is used both for lubrication and cooling for parts such as the pistons.

1.2 Internal combustion engine basics

Internal combustion (IC) engines come in a variety sizes and configurations. Their main purpose is to extract the energy of an combustion process happening inside the engine, hence the name internal combustion engine. The most common configuration utilizes a piston moving up and down inside a cylinder bore, and some valve system to exchange the exhaust and air. The type of engine, two or four stroke determines the valve configuration.

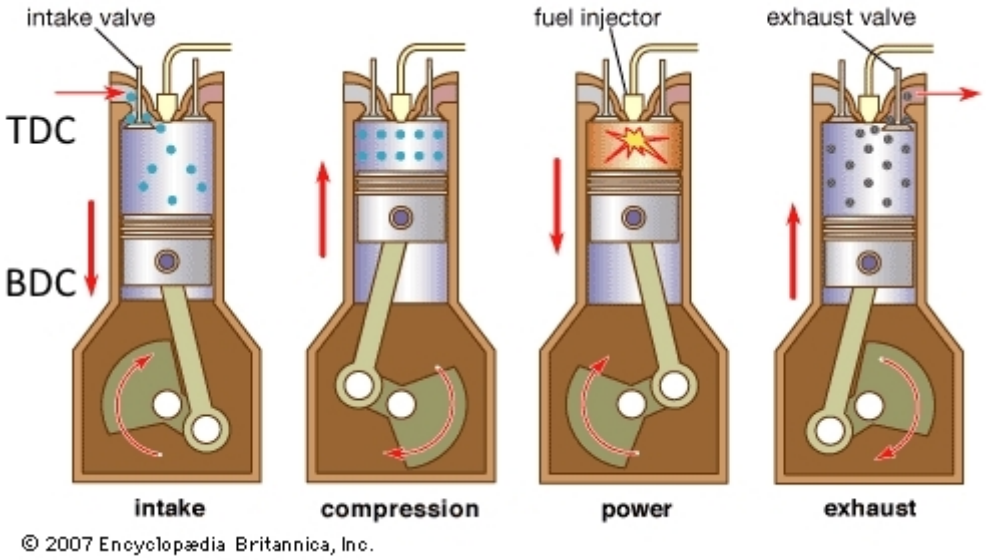

FIGURE 1.2: Internal combustion process (Encyclopedia Britannia 2007)

1.2.1 How the IC process works

A four stroke diesel cycle works as follows:

1. The piston starts at TDC, the intake valve opens and piston moves towards BDC. Air is sucked into the cylinder.
2. The intake valve closes, and the piston moves towards TDC, high compression heats the entrapped air.
3. At TDC the injector sprays diesel into the chamber. The hot compressed air ignites the fuel and the pressure rises. The piston moves towards BDC extracting the energy from the gas expansion.

4. At BDC the exhaust valve opens, the piston moves towards TDC expelling the combusted gases. The process is then repeated.

1.3 The parts in the motor

Engines can be single or multi cylinder in many configurations. For the purpose of this thesis, we will analyze only one cylinder bank. The parts of significance is listed in this section. A complete assembly figure can be seen in **Appendix B**.

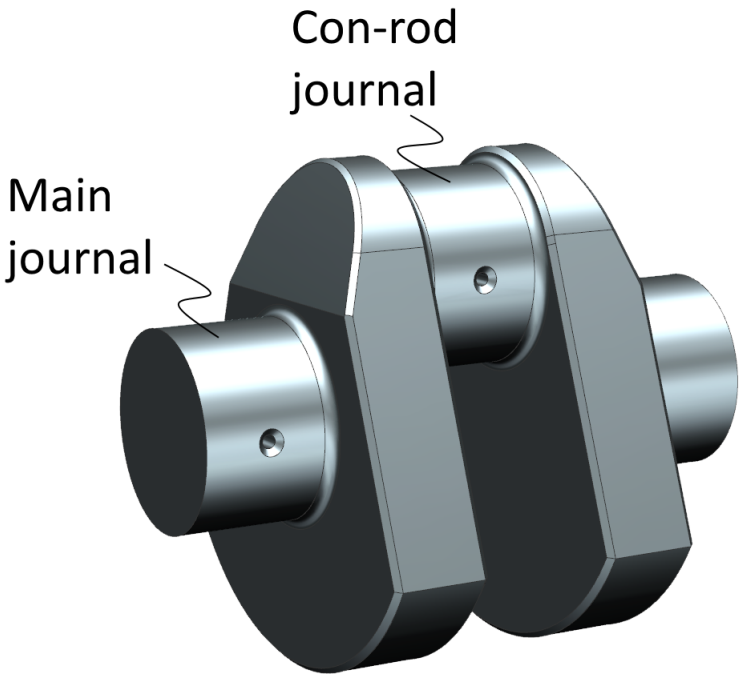

FIGURE 1.3: Crankshaft, for single cylinder. (CAD Model)

1.3.1 The crankshaft

The crankshaft is a machined solid piece of forged steel. The main journal rotates in the main bearing, connecting the piece to the engine block. The con-rod journal is where the connecting rod mounts. Drilled oil channels, **Figure 6.7** connect the main journal to the big-end journal. The channels can have various configurations.

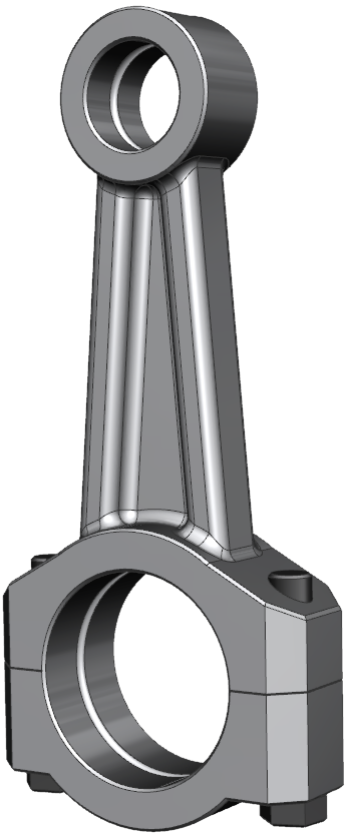

FIGURE 1.4: The connecting rod. (CAD Model)

1.3.2 The connecting rod

The connecting rod connects the crankshaft to the piston. It will encounter high dynamical loads from the rapid back and forth motion. The length of the rod is between the two centres. Bearing cups **Figure 1.5** is used for low friction rotation. An oil channel is drilled between the two centres **Figure 6.12**, these channels can also have various configurations.

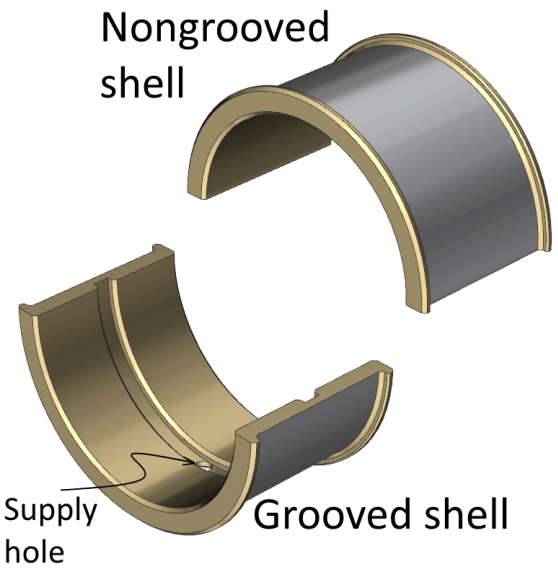

FIGURE 1.5: Hydrodynamic bearing are splitted into two cups to make assembly possible. (CAD Model)

1.3.3 The bearings

Hydrodynamic non-contact bearings is used at the connecting rod small-end and big-end, as well as in the main bearing. For these bearings to work, a constant supply of oil is needed. The bearings have a open track in the centre that goes partly or all around its circumference. At the main bearing, the oil will enter the tracks through the supply hole and lubricate the bearing. The rest will enter the crankshaft leading to con-rod journal through the channels. From here it will lubricate and supply oil to the connecting rod.

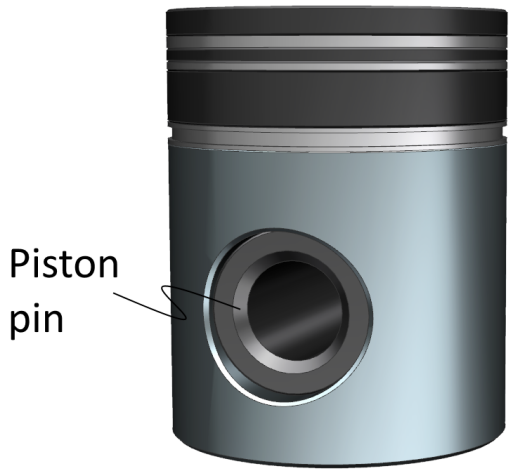

FIGURE 1.6: Pistons. (CAD Model)

1.3.4 The piston

The piston in the engine is the part that allow for energy extraction by volumetric expansion. Many sizes and variations exists, **Figure 1.6**. It has to withstand/reject heat and tolerate high temperatures from the combustion process on the top crown. An piston pin connects the piston to the connecting rod through the hole in the middle of it.

1.3.5 Medium sized engines in generator applications

For electric power production, the engine is in most cases connected directly to the generator without any gearing **Figure 1.1**. The generator will be controlled to run at a speed of 750 RPM to output the alternating current in the correct frequency (50 or 60 Hz). It will start and run for some seconds at lower speeds. When oil pressure is sufficient, the motor accelerates to its operating speed. **Table 1.1** lists some general factors on medium size engines.

Engine speed	750 RPM
Connecting rod length	0.8 m
Crankshaft radius	0.2 m
Piston diameter	0.3-0.4 m

TABLE 1.1: Medium sized engine parameters

Chapter 2

Litterature review

2.1 Piston cooling principles

Piston cooling is generally used high performance and forced induction engines. It is a simple way to control the temperature of the piston to avoid overheating. Many principles for oil cooling of pistons exist, the variations exists mainly due to the size and running speed of the motor. Small motors such as motors used in personal vehicles usually have an nozzle mounted to the block. This is possible due to the smaller stroke of the motor. Large and slow running motors used for marine propulsion may have various extra mechanisms of tubes or rails to deliver oil to the pistons for more consistent flow. Medium sized motors, as considered in this thesis, however deliver the oil through the crankshaft and then the connecting rod **Figure 2.1**. Having a block mounted under-spray solution would demand for a high energy oil delivery for the longer spray for the longer stroke, loosing overall efficiency of the motor.

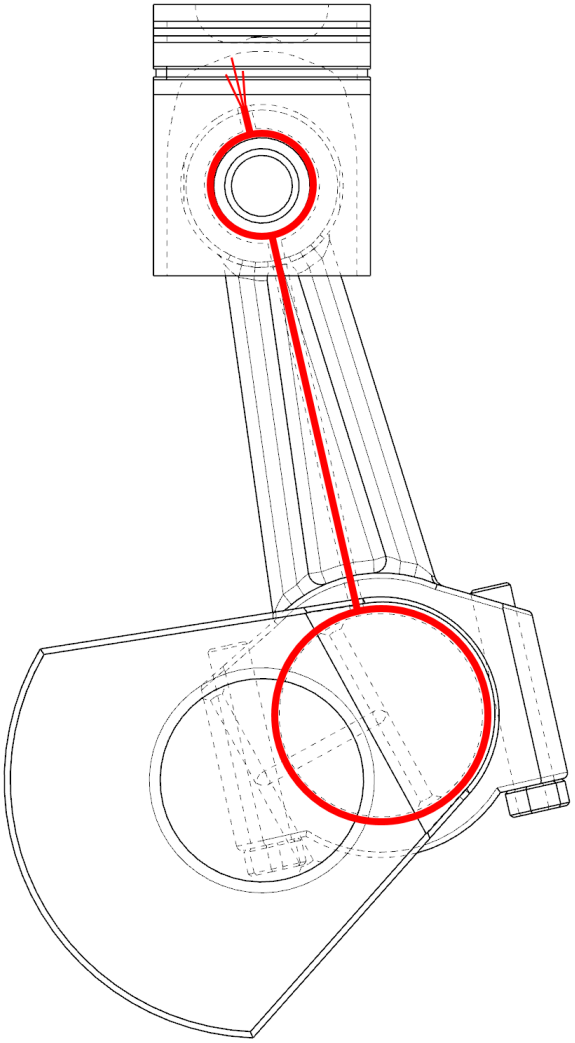

FIGURE 2.1: Oil channels in the con-rod with the nozzle on top cooling the piston. Note that the crankshaft channels is not highlighted.

2.1.1 Previous research on the topic

Previous research has been done on predicting the transient lubricating flow through the crank system. **Kang [3]** predicts the possibility of cavitation in the connecting rod. Other publications such as **Chun [4]** focuses on modelling the complete lubrication system. His research is helpful for understanding the lubrication system of engines. For modeling the transient flow in the connecting rod, **Lebrun [2]**, **Wylie [7], Pedersen [1]** is helpful.

2.1.2 Kang, Transient oil flows within the connecting-rod

Kang uses a the characteristics method for modeling of the channels in the connecting rod on a medium sized diesel engine. His results shows that the oil channel size in the connecting-rod is critical, and discusses the possibility of installing a orifice to control the transient flow. An other important factor he discuss is the difficulty modelling the oil drained by the bearings, as well as the oil transport through them. His results is great for comparing with the model built in this thesis.

2.1.3 Chun, Network analysis of an engine lubrication system

Chun models the lubrication network of a automobile engine. He lists useful formulas for calculating an oil jet flow, crankshaft pressure gain, and bearing lulbrication usage. Kang also uses these formulas in his work.

2.2 Summary, important factors

The knowledge gained from Kang and Chun shows that the oil delivery system can be thought of as a network of resistors. The oil pressure will drop for each resistor it passes. If the crankshaft flow resistance is large, the pressure in the rest of the system will be low. The result is more transient flow and higher possibility of cavitation when the connecting rod moves. To avoid cavitation, the pressure drop throughout the system should be small. It is also important that the bearings do not use excessive amounts of oil, as this will drop the pressure.

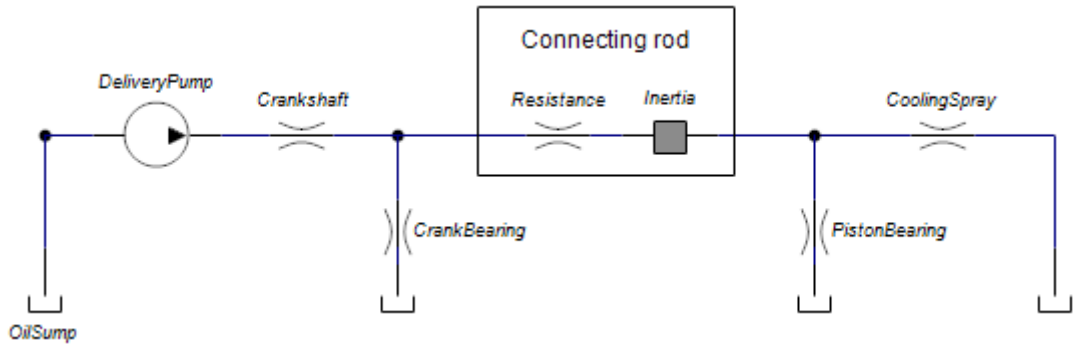

FIGURE 2.2: Simplified network model (20-sim model)

The oil supply pressure in the connecting rod should be as high as possible, this can be achieved by:

1. Having a low flow resistance through the *Crankshaft*.
2. Having a *CrankBearing* that uses as little oil as possible to make sure more oil goes to the con-rod.

The inertia of the oil in the con-rod should not resonate with the movement, this can cause cavitation and excessive lubrication usage. To prevent this:

1. The inertia of the fluid in the channels should be tuned for a frequency different from the oscillatory motion.
2. Extra resistance in the channels can be used to dampen the fluid motion. However it should not restrict the flow.

Chapter 3

Dynamic model

3.1 The piston-crank mechanism

The piston is connected to the rotating crankshaft via an connecting rod. When the crankshaft rotates, the piston displaces an length equal to double the crankshaft stroke radius R. However due to the fact that the connecting rod not being infinitely long, the piston movement becomes complicated.

3.1.1 Modelling the movement of the system

Figure 3.1 shows an geometric view of the mechanism. The connecting rod is connected to the crankshaft in B, and then to the piston in C. This forces the connecting rod to move like a swinging pendulum that is also moved up and down. Modelling the movement, we need to know the piston kinematics x_p, v_p a_p as well as the rod angle α and $\dot{\alpha}$

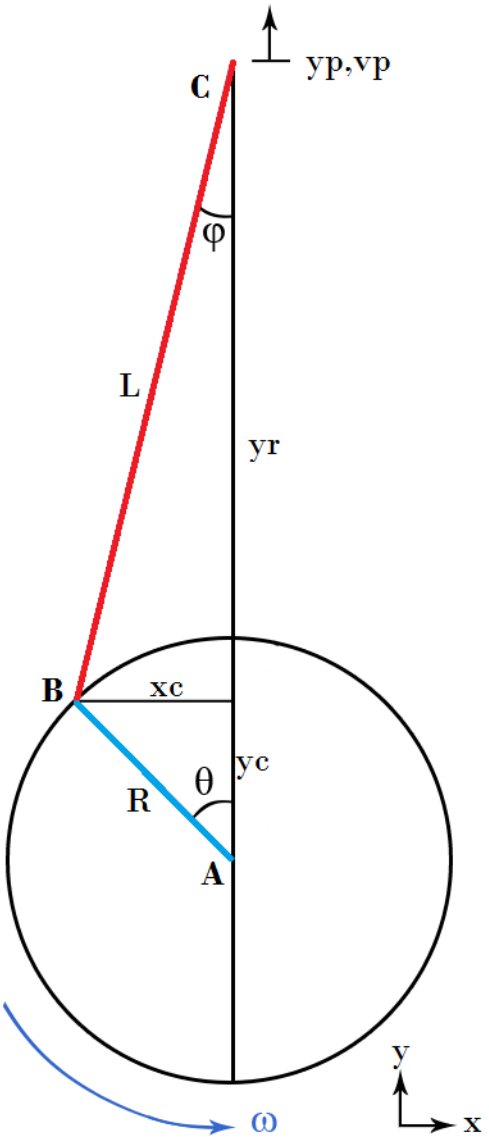

FIGURE 3.1: Crank mechanism. Red connecting rod, blue crankshaft

3.1.2 Piston kinematics

From a geometric view, the position of the piston is:

$$y_p = yc + yr = R\cos\theta + \sqrt{L^2 - R^2\sin^2\theta} \tag{3.1}$$

Using the chain rule to differentiate y_p with respect to time, we get the piston velocity v_p.

$$v_p = \frac{d}{dt}(R\cos\theta + \sqrt{L^2 - R^2\sin\theta}) = -R\dot{\theta}\sin\theta - \frac{R^2\dot{\theta}\sin(\theta)\cos(\theta)}{\sqrt{L^2 - R^2\sin^2\theta}} \tag{3.2}$$

Utilizing the trigonometric identity; $\sin\theta\cos\theta = \frac{1}{2}\sin 2\theta$. The equation is simplified:

$$v_p = -R\dot{\theta}\sin\theta - \frac{R^2\dot{\theta}\sin(2\theta)}{2\sqrt{L^2 - R^2\sin^2\theta}} \tag{3.3}$$

Differentiating one more time with the chain and product rule, we get the piston acceleration a_p.

$$a_p = \frac{d}{dt}v_p \tag{3.4}$$

$$= \frac{d}{dt}\Big(- R\dot{\theta}\sin\theta - \frac{R^2\dot{\theta}\sin 2\theta}{2\sqrt{L^2 - R^2\sin^2\theta}}\Big) \tag{3.5}$$

$$\begin{aligned} &= -R(\ddot{\theta}\sin\theta + \dot{\theta}^2\cos\theta) \\ &\quad - \frac{R^2}{2}\Big(\frac{2\dot{\theta}^2\cos 2\theta}{\sqrt{L^2 - R^2\sin^2\theta}} + \sin 2\theta\Big(\frac{\ddot{\theta}}{\sqrt{L^2 - R^2\sin^2\theta}} - \frac{R^2\dot{\theta}^2\sin\theta\cos\theta}{(L^2 - R^2\sin^2\theta)^{3/2}}\Big)\Big) \end{aligned} \tag{3.6}$$

Again, by using the trigonometric identity; $\sin\theta\cos\theta = \frac{1}{2}\sin 2\theta$ gives:

$$\begin{aligned} a_p &= -R(\ddot{\theta}\sin\theta + \dot{\theta}^2\cos\theta) \\ &\quad - \frac{R^2}{2}\Big(\frac{2\dot{\theta}^2\cos 2\theta}{\sqrt{L^2 - R^2\sin^2\theta}} + \frac{\ddot{\theta}\sin 2\theta}{\sqrt{L^2 - R^2\sin^2\theta}} + \frac{R^2\dot{\theta}^2\sin^2 2\theta}{2(L^2 - R^2\sin^2\theta)^{3/2}}\Big) \end{aligned} \tag{3.7}$$

Note that the engine speed ω contributes squared in $[\dot{\theta}^2\cos\theta]$. $[\frac{R^2}{2}]$ will modulate the main shape of the curve with the $[sin(2\theta)]$ for it to have a tooth looking shape **Figure 3.3**. From now on we will just refer to a_p as a_p.

3.1.3 Rod kinematics

We know the length of the rod L, and $x_c = R\sin\theta$. We can find α:

$$\alpha = \arcsin\left(\frac{R\sin\theta}{L}\right) \tag{3.8}$$

$\dot{\alpha}$ is found by differentiating in time:

$$\dot{\alpha} = \frac{d}{dt}\alpha = \frac{R}{L}\frac{\dot{\theta}\cos\theta}{\sqrt{1-\frac{R^2\sin^2\theta}{L^2}}} \tag{3.9}$$

3.1.4 Acceleration along the axis of the connecting rod

The oil in the connecting rod flows from B to C. Thus we want to know the acceleration in the rod along this axis. As said before, the con-rod swings like an pendulum moving up and down. Thus we get two contributions to the acceleration along the axis of the rod. The earth gravity is neglected.

$$ax_r = ax_{r1} + ax_{r2} \tag{3.10}$$

The dot product of the piston acceleration a_p and the connecting rod angle α gives the axial acceleartion in the connecting rod.

$$ax_{r1} = a_p\cos\alpha \tag{3.11}$$

The second contribution; we know that the centripetal acceleration: $a_c = r\omega^2$, setting $\omega = \dot{\alpha}$ and $r = x_r$ where x_r is the distance from C to B:

$$ax_{r2} = x_r\dot{\alpha}^2 \tag{3.12}$$

The contribution is linearly increasing with x_r. Setting $x_r = \frac{1}{2}L$, the average is found. The total axial acceleration in the rod is then:

$$ax_r = a_p \cos\alpha + \frac{L}{2}\dot{\alpha}^2 \tag{3.13}$$

3.2 Plotting the equtaion

The resulting equations is pretty comlex, plotting the equation in Matlab is done to give an visual idea of the shape of the curve. **Figure 3.2** shows a plot of an medium sized engine, the curves are quite smooth. The frequency of the waves is at 750 RPM is 12.5Hz. The contribution from the rod rotation is rather small.

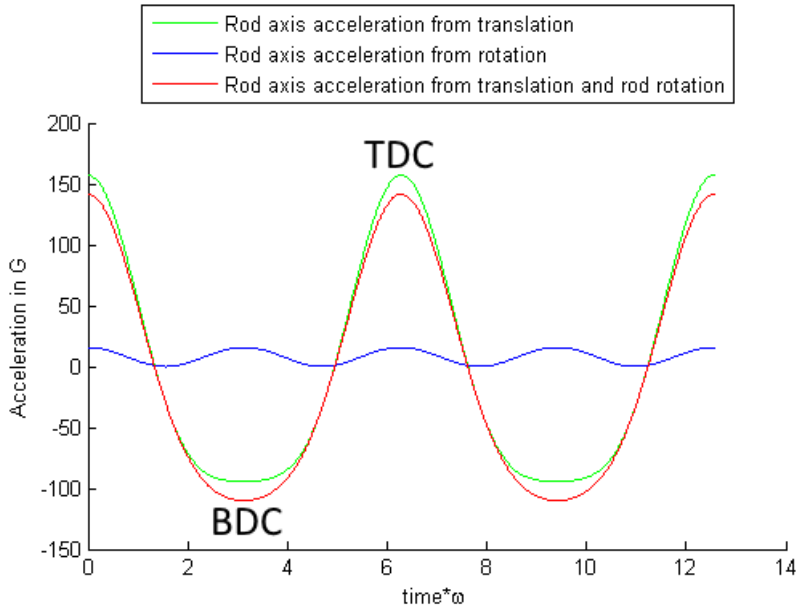

FIGURE 3.2: Plotting the acceleration along the axis of the con-rod. L=0.8m R=0.2m

Replacing the con-rod by an shorter one **Figure 3.3**. The translation component changes and the rotation component becomes larger. However they seem to counteract since the total contribution is approximately the same.

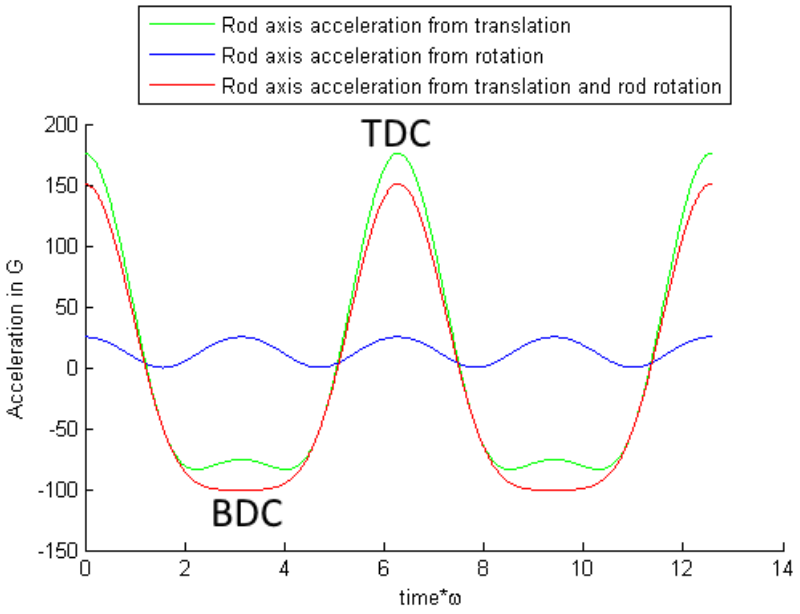

FIGURE 3.3: L=0.5m R=0.2m

3.3 Summary

The dynamic model will be used to define the acceleration along the connecting rod axis. Assuming the fluid in the connecting rod channel **Figure 6.12** can be thought of as an "lumped section". According to **Wylie [7]**, this is accurate when the length of the tube is 0.04 the wavelength of the oscillatory motion through the medium:

$$\lambda = \frac{c}{f} = \frac{1460m/s}{12.5Hz} = 116.8m \tag{3.14}$$

The rod channel length r_{crc} of 0.8 m is 0.0086 of λ, thus we can assume a lumped section. c and r_{crc} listed in table **Table 7.1**. The resulting pressure momentum from the exerted acceleration on the tube:

$$\Delta P = ax_r \cdot \rho \cdot L_{crc} \tag{3.15}$$

Chapter 4

Bond graph introduction

4.1 Introduction

A very powerful method for modelling dynamical systems is the *bond graph language*. Basically it is a systematic way of modelling in terms of energy, the visual bond-graph is used to develop the differential equations through a set of rules. It can be used to model and couple together dynamical systems on many physical disciplines, **Table 4.1**. The visual approach also gives an intuition of the dynamic behaviour of the system.

Energy domain	**Effort** e	**Flow** f	**Momentum** p	**Displacement** q
Mechanical translation	Force [F]	Velocity [m/s]	Linear momentum [Kgm/s]	Distance [m]
Mechanical rotation	Torque [Nm]	Angular velocity [rad/s]	Angular momentum [Nms]	Angle [rad]
Hydralulic	Pressure [Pa]	Volume flow rate [m^3/s]	Pressure momentum [N/m^2s]	Volume [m^3]
Electrical	Voltage [V]	Volume Current [A]	Flux linkage [Vs]	Charge [As] or [C]

TABLE 4.1: Bond graph can be used to model on several physical diciplines

4.2 Bond graph modelling example

An example of a hydraulic system is seen in **Figure 4.1**. A oil pump delivers an oil flow to the system. A common pressure node attaches an accumulator and a long section of pipe with an flow resistor at the end. From here the oil leaves to the reservoir with an atmospheric pressure.

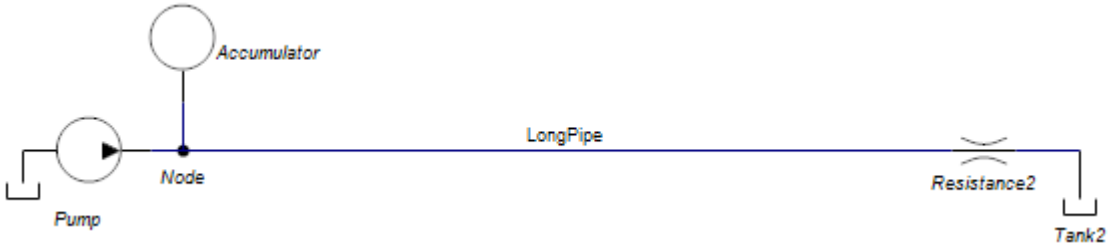

FIGURE 4.1: Hydraulic system example. (20-sim model)

4.2.1 The elements

The basic elements I, C , R of the bond graph method is given in **Table 4.2**. These elements will represent the physical properties of the system. The two other *Sf* and *Se* are active elements which is used to input energy to the system. At last the *transformer* and the *Gyrator* can be used for domain boundaries, gear ratios or turbines.

Element	Description	Function	Description	Symbol
R	Resistor	Dissipates energy	Fricition	
I	Inertia	Kinetic energy storage	Lumped mass	
C	Capacitor	Potential energy storage	Volume elasticity	
Sf	Set flow	Defines an flow	A set flow	
Se	Set effort	Defines an effort	A set pressure	
1	1 Junction	Common flow	Sum of effort is zero	**1**
0	0 Junction	Common effort	Sum of flow is zero	**0**
TF	Transformer	Multiplication factor	Gears, hyd cylinders	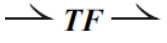
GY	Gyrator	Gyration factor	Turbine, centrifuge	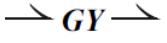

TABLE 4.2: Bond graph basic elements

4.2.2 Model development

For modelling the example, we use an set flow to model the pump, it connects to the node where the pressure is equal at all branches. However in the node, each flow is different. A zero-junction will define a common pressure, and sum for the all the flows. From here the oil enters the long pipe. The flow in the pipe is constant over its length, but the pressure may vary from end to end due to the inertia forces of the fluid in the pipe. An one-junction maps for a constant flow and sums the pressure, it connects with the inertia junction. After the long pipe the oil enters an resistor that defines the flow through the second one-junction. The atmospheric pressure at the end is set by an set effort junction.

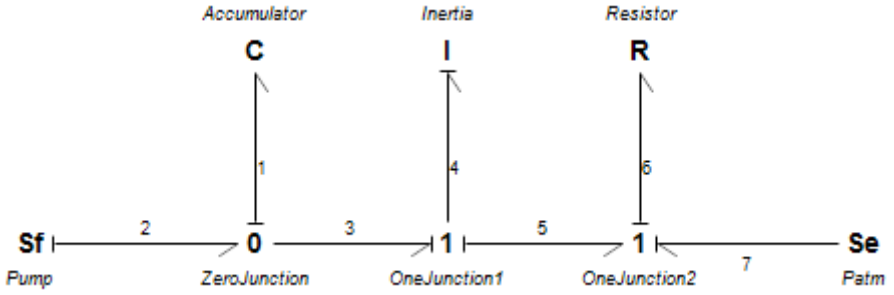

FIGURE 4.2: Hydraulic system bond-graph (20-sim model)

Figure 4.2 Show the bond graph of the hydraulic system in **Figure 4.1**. The elasticity of the oil in the long pipe was neglected.

4.2.3 The powerbond

In an dynamic system, the energy will exchange between potential and kinetic energy and then dissipate as friction. Power is generally:

$$P = Force \cdot Velocity = effort \cdot flow \tag{4.1}$$

Energy flow, or power direction is visualized with the half tip arrow called a *Powerbond*. It connects the other elements in the graph and contains a value for the *effort* and *flow*. Causality on the powerbond is assigned from causality rules, **Pedersen, Engja [5]** and is illustrated with an flat end. The flat end defines effort, the other end defines flow. This is important for developing the state equations.

4.3 Developing the equations

The two state variables of the system is the momentum of the inertia element I, and displacement of the capacitive element C. The following terms is developed from constitutive rules in **Appendix A**, and is used to develop the equations.

ZeroJunction : The effort is the same at all branches, but it is defined by *powerbond 1* coming from the C element. The flow at this junction will be: $f_2 - f_1 - f_3 = 0$

OneJunction1 : The flow is constant for all branches and defined by *powerbond 4* coming from the I element. The effort at this junction is: $e_3 - e_4 - e_5 = 0$

OneJunction2 : flow is constant and defined by *powerbond* 5, the effort is: $e_5 - e_6 + e_7 = 0$

I element : $q = Ce$

C element : $p = If$

R element : $e = Rf$

4.3.1 The equations

The state equations can be written on a matrix form where **A** contains the values of the I, C and R elements. **x** and **u** is state variables and **B** is a coupling matrix.

$$\dot{\mathbf{x}} = \mathbf{A}\mathbf{x} + \mathbf{B}\mathbf{u} \tag{4.2}$$

The inertia element:

$$\begin{aligned} \dot{x_1} = \dot{p_4} &= e_4 \\ &= e_3 - e_5 \\ &= e_1 - (e_6 - e_7) \\ &= \frac{q_1}{C_1} - (R_6 f_6 - Se_7) \\ &= \frac{q_1}{C_1} - (R_6 f_5 - Se_7) \\ &= \frac{q_1}{C_1} - (R_6 f_4 - Se_7) \\ &= \frac{q_1}{C_1} - (R_6 \frac{p_4}{I_4} - Se_7) \end{aligned} \tag{4.3}$$

The capacitive element:

$$\begin{aligned} \dot{x_2} = \dot{q_1} &= f_1 \\ &= f_2 - f_3 \\ &= Sf_2 - f4 \\ &= Sf_2 - \frac{p_4}{I_4} \end{aligned} \tag{4.4}$$

The resulting set of equations on matrix form:

$$\begin{bmatrix} \dot{x_1} \\ \dot{x_2} \end{bmatrix} = \begin{bmatrix} -\frac{R_6}{I_4} & \frac{1}{C_1} \\ 0 & -\frac{1}{I_4} \end{bmatrix} \begin{bmatrix} x_1 \\ x_2 \end{bmatrix} + \begin{bmatrix} 1 & 0 \\ 0 & 1 \end{bmatrix} \begin{bmatrix} Se_7 \\ Sf_2 \end{bmatrix} \tag{4.5}$$

4.4 Summary

As seen, the bond graph results in a set of equations that can be solved in matlab etc. Another option is to use bond-graph purpose software such as 20-sim. This software can assign the causality, develop and solve the state equations.

Chapter 5

Pipe transient fluid modeling

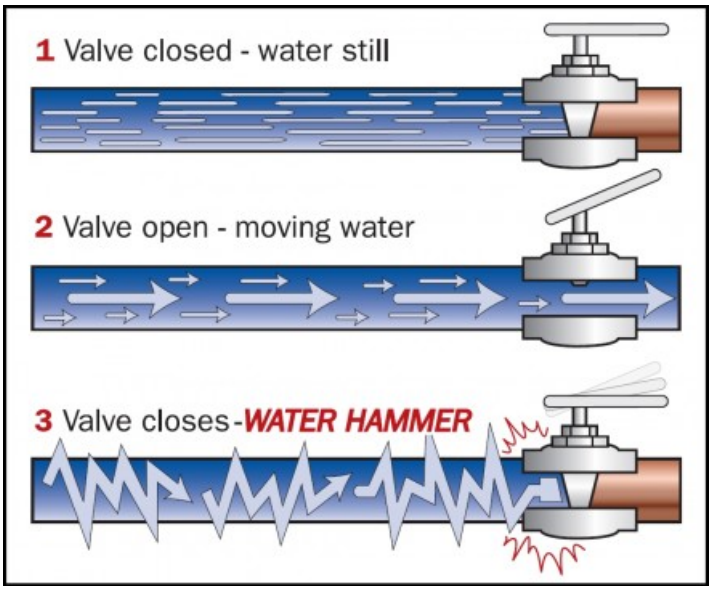

FIGURE 5.1: Water hammer illustration (www.zillow.com)

5.1 Introduction

Having a long sections of tubes and intermittent flow invites for some dynamical effect so called the "Water hammer effect". If sudden change to the flow occurs, pressure waves will propagate through the tube. Problems such as cavitation and breaking water pipes can occur. Likewise, the change in flow is delayed if the pressure is suddenly changed in one end. The "water hammer" phenomena is well documented and a lot of theory has been written about the subject in engineering journals. In this chapter, we will build the

necessary equations for representing the intermittent flow in the connecting rod based upon modal analysis. **Lebrun [2]** models for the modal representation of pipe flow, and it is possible to input the pressure changes from the tube movement.

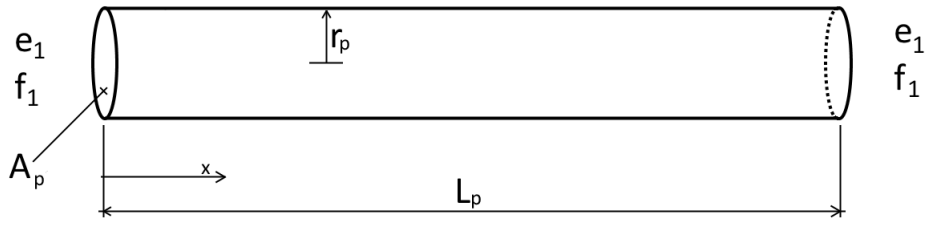

FIGURE 5.2: Fluid transmission line. Uniform cross sectional area A_p, length L_p raduis r_p

5.1.1 Basic equations

Following **Lebrun [2]**. The flow of a compressible fluid in a pipe is described by the momentum and continuity equation.

Momentum equation:

$$\frac{1}{\rho}\frac{\partial e}{\partial x}\cdot\frac{1}{A_p}\frac{\partial f}{\partial t}+R_f\frac{f}{A_p}=0 \tag{5.1}$$

Continuity equation:

$$\frac{c^2}{A_p}\frac{\partial f}{\partial x}+\frac{1}{\rho}\frac{\partial e}{\partial t}=0 \tag{5.2}$$

Where

- e is pressure [Pa]
- f is the flow-rate [m^3/s]
- ρ is the density of the fluid [Kg/m^3]
- A_p is the cross-sectional area of the pipe
- R_f is the Hagen-Poisuille loss coefficient

5.1.2 Combining the basic equations

Combining the momentum and continuity equations, flow or pressure can be eliminated. A rigid pipe is assumed.

Pressure eliminated:

$$\frac{\partial f^2}{\partial t^2} + R_f \frac{\partial f}{\partial t} - c^2 \frac{\partial f^2}{\partial x^2} = 0 \tag{5.3}$$

Flow eliminated:

$$\frac{\partial e^2}{\partial t^2} - R_f \frac{\partial e}{\partial t} - c^2 \frac{\partial e^2}{\partial x^2} = 0 \tag{5.4}$$

For modelling the friction forces, laminar flow is assumed. The Hagen-Poiseuille Friction equation, **White [6]** is used. The loss coefficient R_f:

$$R_f = \frac{8\nu}{r_p^2} \tag{5.5}$$

Where

- ν is the kinematic fluid viscosity
- r_p is the radius of the pipe

5.1.3 Solving by separation of variables

We are interested in **Equation 5.3**, it is a damped one-dimensional wave equation. We separate the variables, and the solution is on the form:

$$f(x,t) = \sum_{i=0}^{\infty} G_i(x)\eta_i(t) \tag{5.6}$$

It can then be separated into the following two equations:

$$\ddot{\eta}_i + R_f \dot{\eta}_i - \mu \eta_i = 0 \tag{5.7}$$

$$c^2 G_i'' - \mu G_i = 0 \tag{5.8}$$

For $\mu = -\omega^2$ the solution will be on the following form, note that the solution in time will be solved numerically and is therefore noted as just $\eta_i(t)$

$$\sum_{i=0}^{\infty} G_i(x)\eta_i(t) = \Big(Asin(\frac{\omega_i}{c}x) + Bcos(\frac{\omega_i}{c}x)\Big) \cdot \eta_i(t) \tag{5.9}$$

The flow gradient at the pipe ends is zero. Mathematically this means $G_i^{'}(0) = G_i^{'}(L_p) = 0$, yielding $A = 0$ and $\omega_i = \frac{i\pi c}{L_p}$ respectively. To normalize the mode shapes, $B = 1$. The solution with the natural frequency is as follows:

$$f(x,t) = \sum_{i=0}^{\infty} G_i(x)\eta_i(t) = cos(\frac{\omega_i}{c}x) \cdot \eta_i(t) \tag{5.10}$$

$$\omega_i = \frac{i\pi c}{L_p} \tag{5.11}$$

Substituting 5.6 into 5.3 and adding the input pressure at the ends yields:

$$\frac{\rho}{A_p}\Big(\sum_{i=0}^{\infty} G_i\ddot{\eta}_i + R\sum_{i=0}^{\infty} G_i\dot{\eta}_i - c^2\sum_{i=0}^{\infty} G_i^{''}\eta_i\Big) = \dot{e}_1\delta(0) - \dot{e}_2\delta(L_p) \tag{5.12}$$

Where δ is the delta dirac function. Multiplying both sides by G_i and integrating over the length L_p:

$$\frac{\rho}{A_p}\Big(\sum_{i=0}^{\infty}\int_0^{L_p} G_i^2\ddot{\eta}_i dx + R\sum_{i=0}^{\infty}\int_0^{L_p} G_i^2\dot{\eta}_i dx - c^2\sum_{i=0}^{\infty}\int_0^{L_p} G_iG_i^{''}\eta_i dx\Big) = \int_0^{L_p} G_i\Big(\dot{e}_1\delta(0) - \dot{e}_2\delta(L_p)\Big)dx \tag{5.13}$$

From 5.9 we know that $G_i = cos(\frac{\omega}{c}x)$, then:

$$\int_0^{L_p} G_i^2 dx = \int_0^{L_p} cos(i\pi\frac{x}{L_p})^2 dx = \begin{cases} L_p & \text{if } i = 0 \\ \frac{L_p}{2} & \text{else} \end{cases} \tag{5.14}$$

Substituting 5.14 into 5.13 with the fact that: $G_i^{''} = -\frac{\omega_i^2}{c^2}G_i = (\frac{i\pi}{L_p})^2 G_i$ we get two equations:

For i=0:

$$\frac{\rho L_p}{A_p}\sum_{i=0}^{\infty}\ddot{\eta}_i + R_f\frac{\rho L_p}{A_p}\sum_{i=0}^{\infty}\dot{\eta}_i - \frac{\pi^2\rho c^2 i^2}{A_p L_p}\sum_{i=0}^{\infty}\eta_i = G_i(\dot{e}_1\delta(0) - \dot{e}_2\delta(L_p)) \tag{5.15}$$

And for $i = 1, 2, 3, ..., \infty$:

$$\frac{\rho L_p}{2A_p}\sum_{i=0}^{\infty}\ddot{\eta}_i + R_f\frac{\rho L_p}{2A_p}\sum_{i=0}^{\infty}\dot{\eta}_i - \frac{\pi^2\rho c^2 i^2}{2A_p L_p}\sum_{i=0}^{\infty}\eta_i = G_i(\dot{e}_1\delta(0) - \dot{e}_2\delta(L_p)) \tag{5.16}$$

5.1.4 Adapting the equation for Bond graph implementation

Replacing the constant terms on the left side by the values in **Table 5.1** and utilizing $G_i(0) = 1$ and $G_i(L_p) = cos(i\pi) = (-1)^i$ for all i, on the right side:

$$I_i\sum_{i=0}^{\infty}\ddot{\eta}_i + R_i\sum_{i=0}^{\infty}\dot{\eta}_i - C_i^{-1}\sum_{i=0}^{\infty}\eta_i = \dot{e}_1 - (-1)^i\dot{e}_2 \tag{5.17}$$

The pressure momentum, the oil in moving con-rod is assumed a "lumped section" such that $\dot{P_{ar}} = \frac{d}{dt}a_r\rho L_p$.

$$I_i\sum_{i=0}^{\infty}\ddot{\eta}_i + R_i\sum_{i=0}^{\infty}\dot{\eta}_i - C_i^{-1}\sum_{i=0}^{\infty}\eta_i + \dot{P_{ar}} = \dot{P}_1 - (-1)^i\dot{P}_2 \tag{5.18}$$

Integrating in time and using a finite representation:

$$I_i\sum_{i=0}^{n}\dot{\eta}_i + R_i\sum_{i=0}^{n}\eta_i - C_i^{-1}\sum_{i=0}^{n}\int\eta_i dt + P_{ar} = P_1 - (-1)^i P_2 \tag{5.19}$$

5.2 Summary

The bond-graph model representing the pipe section is shown in **Figure 5.3**. This model will calculate the transient flow based upon P_1, P_2 and P_{ar}. It includes the terms from i = 0, 1 and 2. Transformer (TF) elements represents the $(-1)^i$ part. The values of the element is calculated with the equations in **Table 5.1**.

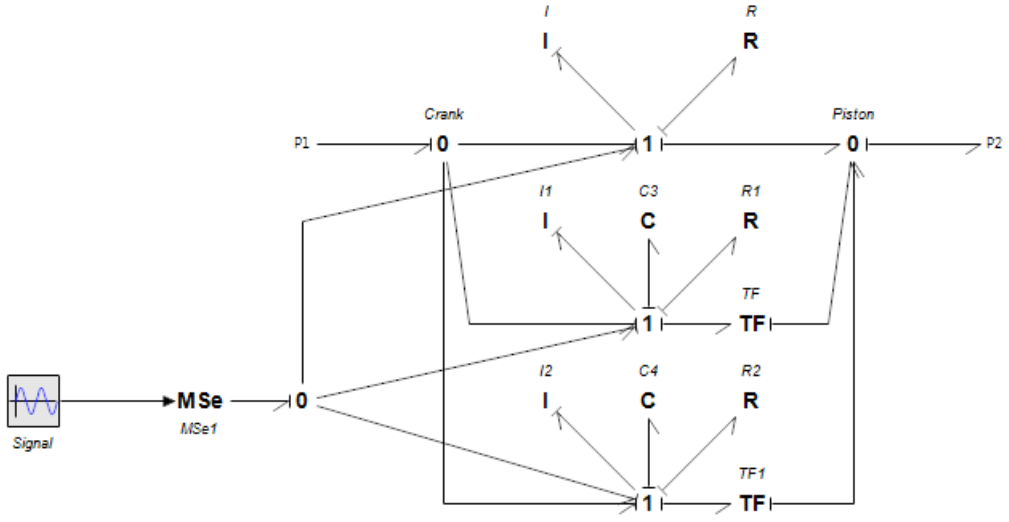

FIGURE 5.3: Bond graph representation for i = 0, 1 and 2. The external force defined by the *MSe* element is controlled by the ax_r signal. (20-sim model)

	I	C	R
$i = 0$	$I_0 = \frac{\rho L_p}{A_p}$	$C_0 = \infty$	$R_0 = R_f \frac{\rho L_p}{A_p}$
$i = 1, 2, ..., \infty$	$I_i = \frac{\rho L_p}{2A_p}$	$C_i = \frac{2A_p L_p}{\pi^2 \rho c^2 i^2}$	$R_i = R_f \frac{\rho L_p}{2A_p}$

TABLE 5.1: Values for the I, C, and R elements of the bond graph

The model is basically a modified version of the the model in **Lebrun [2]**. Note that this model is not valid if cavitation or column separation occurs in the pipe. It also assumes laminar flow and not turbulent.

Chapter 6

Model development

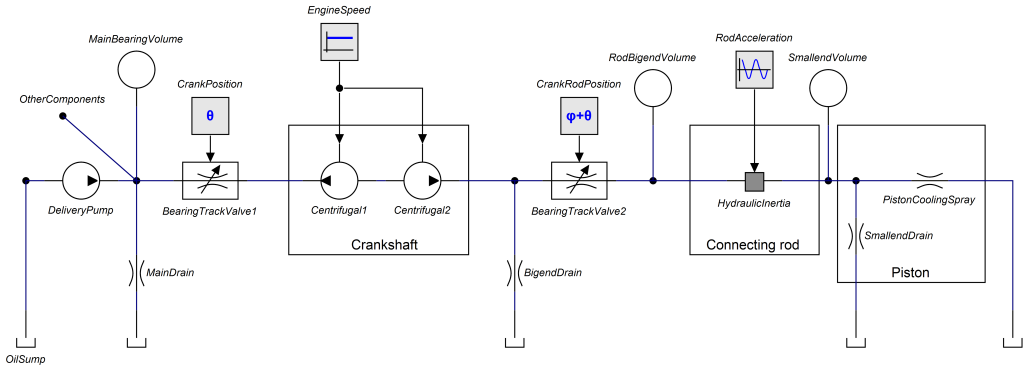

FIGURE 6.1: Oil delivery system (20-sim model)

6.1 Introduction

In this chapter, the sub-models and the final model is built. The hydraulic diagram is shown in **Figure 6.1**. First the oil from the tank enters the *Displacement pump* that also has a pressure control valve inside. From here the oil goes to the *Main bearing*, it has a small *volume* and drain some oil for lubrication. The oil then enters the *Crankshaft* that will amplify the pressure a little. The *Bigend bearing* drain some oil, but the rest of the oil enter the *Connecting rod* that has small *volumes* at the ends. The connecting rod moves rapidly and *inertia forces* are high. When the oil reaches the *Piston*, it will be used for lubrication and for cooling in the nozzle. A bigger version of **Figure 6.1** is shown in **Appendix C**.

6.2 Submodels for the system

The submodels are developed in this section, we start with the oil pump that sucks oil from the oil tank and pressureizes the system. The code implementation for various elements is found in **Appendix E**

6.2.1 Oil delivery pump

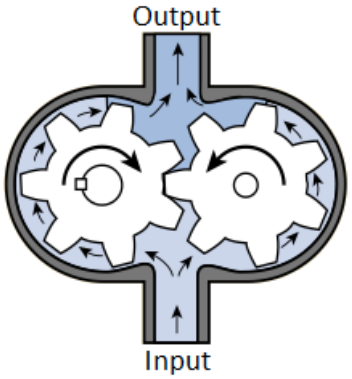

FIGURE 6.2: Displacement pump, the gears pushes the oil through the pump. (www.hydraulicspneumatics.com)

An engine usually have an fixed displacement pump **Figure 6.2** connected to the crankshaft through some gearing system. The flow from the oil pump is ideally proportional to the speed of the input shaft. Resisting the output flow will increase the system pressure. If the flow is blocked totally, the pump can not rotate. At high engine speeds the pump deliver more oil than the engine can use, resulting in a too high pressure. A pressure control valve is used to regulate the pressure. This valve P will open when the hydraulic force $F = PA$ compresses the spring far enough for the oil to escape the little tube, **Figure 6.3**. The result is a constant pressure even if the orifice R is changed, within certain limits notably.

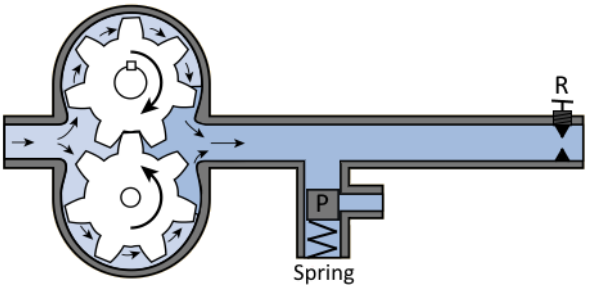

FIGURE 6.3: Displacement pump and relief valve, the relief valve will maintain a constant pressure even if the orifice R is changed. (www.hydraulicspneumatics.com)

This type of regulation would yield an Pressure/engine speed curve like **Figure 6.4**. At lower engine speeds, the pump does not deliver much oil so the pressure will be low. But at higher speeds the pressure control valve will open and control the pressure to P_{set}. At 750 PM we can assume that the delivery pressure is fairly constant. In this thesis, a constant pressure oil delivery will be used. **Figure 6.6** illustrates the submodel.

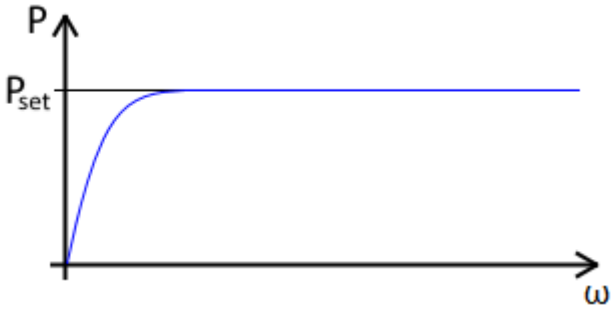

FIGURE 6.4: The pressure is constant at higher engine speeds due to the pressure control valve

6.2.2 Hydraulic volumes

For modelling small hydraulic volumes we use the bulk modulus of the fluid to model for the elasticity of the volume.

$$\beta = -V\frac{\Delta P}{\Delta V} \tag{6.1}$$

Working with the equation, we can implement it into a capacitive element.

$$C = \frac{V}{\beta} \tag{6.2}$$

A capacitive element coupled to a zero junction will model a hydraulic volume. The value of C is calculated with **Equation 6.2**

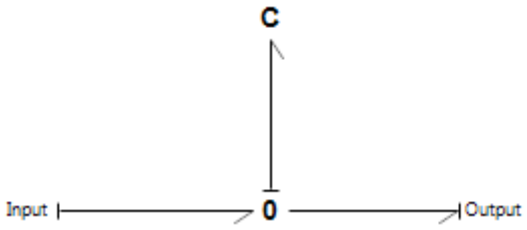

FIGURE 6.5: Hydraulic volume sub-model

6.2.3 Bearings

The hydrodynamic bearings will drain some amount of oil and this will drain to the engine sump. Less oil will then arrive to the cooling nozzle. Equation 14 in **Chun [4]** models for an main bearing flow that will be used to model for all the bearings in the motor. For an bearing with circumferential grooved bearings:

$$q = \frac{\pi c^3 D}{6\nu(L-a)}(2+3\epsilon^2)\Delta P \tag{6.3}$$

Where
- c is the radial clearance [m]
- D is the bearing diameter [m]
- ν is the kinematic viscosity of the lubricant [Pas]
- L is the width of the bearing [m]
- a is the groove width [m]
- ϵ is the eccentricity

An R element can be used to implement the flow used for lubrication in bearings. The R element will input the *effort* as ΔP and then calculate the *flow*. **Figure 6.6** shows how the main bearing R element is implemented.

$$R_{bearing} = \frac{\pi c^3 D}{6\mu(L-a)}(2+3\epsilon^2) \tag{6.4}$$

Table 6.1 shows the calculated values for R. Bearing clearance of 0.01 mm is assumed for all bearings.

	c [mm]	D [mm]	μ [Pas]	L [mm]	a [mm]	ϵ	R [m^3/Pas]
Main bearing	0.01	300	50e-6	200	10	0	3.3e-11
Big end bearing	0.01	300	50e-6	200	10	0	3.3e-11
Small end bearing	0.01	150	50e-6	140	10	0	2.4e-11

TABLE 6.1: Bearing lubrication drain constants

Figure 6.6 illustrates a *Set effort* that defines the input pressure to the main bearing and acts as the supply pump. $Se = P_{set}$. An R element at the main bearing models for the oil drained by the bearing. A volume is also added.

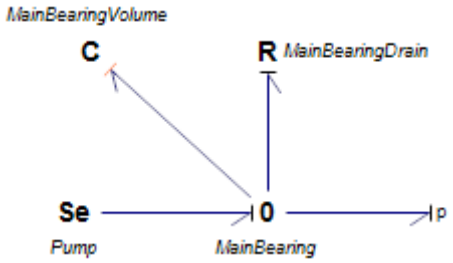

FIGURE 6.6: The bond graph submodel for the oil delivery pump and the main bearing usage.

6.2.4 Crankshaft model

The crankshaft have an channel input that is drilled in the main journal into the centre. From here it goes to the con-rod journal. **Figure 6.7** shows a cross section of the crankshaft with the oil channels in red.

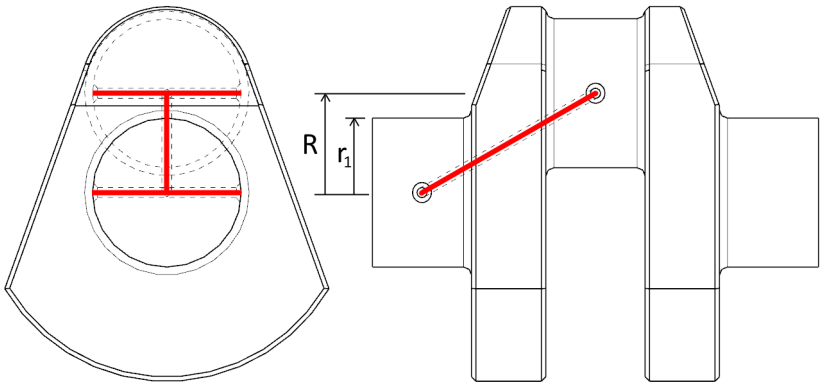

FIGURE 6.7: Crankshaft axial crossection with the oilchannels in red. (NX CAD model)

The oil that enters the main journal is approaching the centre of rotation and will encounter an acceleration field pushing against the flow. However from the centre and to the con-rod journal, the acceleration will push the oil in its flow direction. From Bernoulli we have that $\Delta P = \rho \cdot a \cdot \Delta h$ when the gravitational field is constant. For a varying acceleration field we need to integrate over the length:

$$dP = \rho a(r) dr \tag{6.5}$$

Integrating from r_1 to the origin the pressure gradient is negative. Again, the centripetal acceleration: $a_c = r\omega^2$

$$P = \int_{r_1}^{0} \rho a(r) dr = \int_{r_1}^{0} \rho r \omega^2 dr = \rho \omega^2 [\frac{1}{2} r^2]_{r_1}^{0} = -\frac{1}{2} \rho \omega^2 r_1^2 \tag{6.6}$$

The same procedure from the origin to R, the contribution is positive:

$$P = \int_{0}^{R} \rho r \omega^2 dr = \rho \omega^2 [\frac{1}{2} r^2]_{0}^{R} = \frac{1}{2} \rho \omega^2 R^2 \tag{6.7}$$

The change in pressure from the oil entering at A and leaving B will then be:

$$\Delta P = \frac{1}{2}\rho\omega^2(R^2 - r_1^2) \tag{6.8}$$

The sub model for the crankshaft can be seen in **Figure 6.8**. A *modified set effort* contains **Equation 6.8**. The flow in the crankshaft channels is modelled with inertia I and friction R. These values is calculated based upon **Table 5.1** for $i = 0$ with the crankshaft parameters where $L_{csc} = R + 2R_1$ and r_{csc} for the the channel radius.

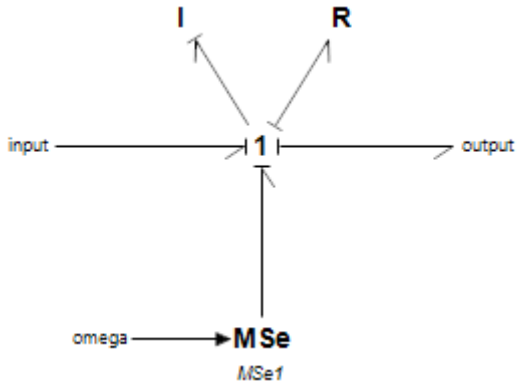

FIGURE 6.8: Crankshaft submodel

6.2.5 Nozzle model

The cooling jet, **Figure 6.14** is made from an nozzle on top of the connecting rod. It should shoot a jet of oil, but not to a point where it atomizes the spray. An ideal spray would look something like a water fountain. When the oil enters the orifice, the closing down area will accelerate the oil, making a jet of oil.

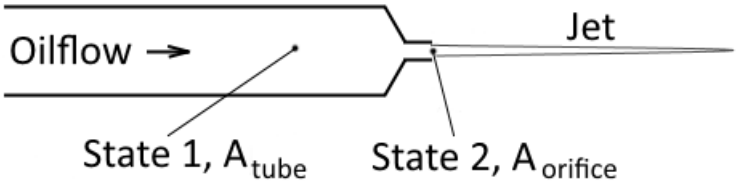

FIGURE 6.9: Nozzle jet illustration

For modelling the jet we use Bernoulli's law. State 1 is within the delivery tube, state 2 is just in the end of the nozzle:

$$\frac{P_1}{\rho} + \frac{1}{2}V_1^2 + gz_1 = \frac{P_2}{\rho} + \frac{1}{2}V_2^2 + gz_2 = constant \tag{6.9}$$

Assuming $z_1 = z_2$ the equation simplifies.

$$\frac{P_1}{\rho} + \frac{1}{2}V_1^2 = \frac{P_2}{\rho} + \frac{1}{2}V_2^2 = constant \tag{6.10}$$

Then setting $P_1 - P_2 = \Delta P$. Where ΔP is the pressure difference from the oil supply to the atmosphere.

$$\frac{\Delta P}{\rho} + \frac{1}{2}V_1^2 = \frac{1}{2}V_2^2 = constant \tag{6.11}$$

Also assuming $V_1/V_2 < 1$, then $V_1^2/V_2^2 << 1$. Thus we can assume that $V_1 = 0$. V_2 is then set to V for simplicity.

$$\frac{\Delta P}{\rho} + \frac{1}{2}V^2 = constant \tag{6.12}$$

Rearranging and setting $constant = K_d$ where K_d is a discharge coefficient, we get the velocity of the fluid leaving the orifice. K_d is used to calibrate the nozzle according to the pressure difference ΔP and the geometry of the orifice.

$$V = K_d\sqrt{\frac{2\Delta P}{\rho}} \tag{6.13}$$

To find the flow we simply use that $f = VA$ then

$$f = K_d A_{orifice}\sqrt{\frac{2\Delta P}{\rho}} \tag{6.14}$$

The result is similar to the oil jet flow equations given in **Chun [4]** and **Lebrun [2]**. An R element will be used in the model:

$$f = R_{Nozzle} \cdot \sqrt{abs(e)} \cdot sign(e) \tag{6.15}$$

Here $abs(e)$ is used to make sure the solution does not go complex. $sign(e)$ was then used to bring back the sign of e.

$$R_{Nozzle} = K_d A_d \sqrt{\frac{2}{\rho}} \tag{6.16}$$

A_d is set to a constant such that we can use K_d to inut the cooling flow in l/min. Assuming we want a cooling rate of 1 l/min. The average pressure in the rod is assumed 4 bar:

$$A_d = \frac{1/60000}{\sqrt{\frac{2 \cdot 4 \cdot 10^5}{800}}} = 5.27 \cdot 10^{-7} \tag{6.17}$$

The nozzle is modeled with a R element containing **Equation 6.15**. **Figure 6.10** shows the bondgraph submodel for the piston with the cooling nozzle and bearing drain R element.

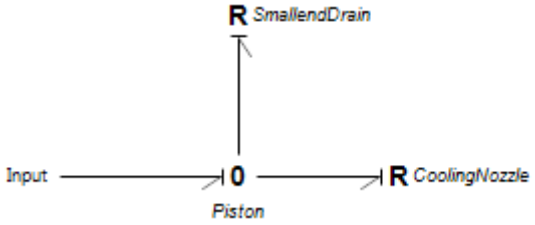

FIGURE 6.10: Piston node with the lubrication R and nozzle R elements

6.2.6 Bearing track valves and flowthrough loss

In some engines the bearing tracks in the hydrodynamic bearings does not go all the way around. The result will be a intermittent delivery through the bearing. This can be modeled with a resistive element defining the flow through an 1-junction. For the closed channel it is high in general, resisting the flow. For the open channel, the pressure loss can be calculated with Equation 1 in **Kang [3]**:

$$\Delta P = KV^2 \tag{6.18}$$

Where:
- Δ P is the pressure loss [Pa]
- K is a loss coefficient
- V is the velocity of the fluid [m/s]

Modifying the equation for the bond-graph implementation, velocity V is converted to flow f. Then $R_{loss} = \frac{K}{A_{channel}}$. The values of R_{loss} is collected from Kang.

$$e = R_{loss} \cdot f^2 \cdot sign(f) \tag{6.19}$$

The submodel has resistive elements defines the flow of the 1-junction. The *Control* signal is calculated from θ on the main bearing and $\theta + \alpha$ for the big-end bearing. R_{Loss} element contains **Equation 6.19**. Code implementations is seen in **Figure E.3** and **Figure E.4**.

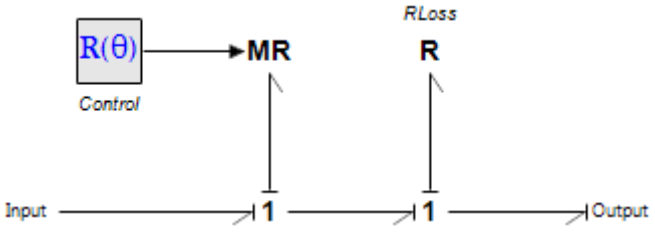

FIGURE 6.11: Bearing flow-through loss with control signal for controlling the valve

6.2.7 Connecting rod model

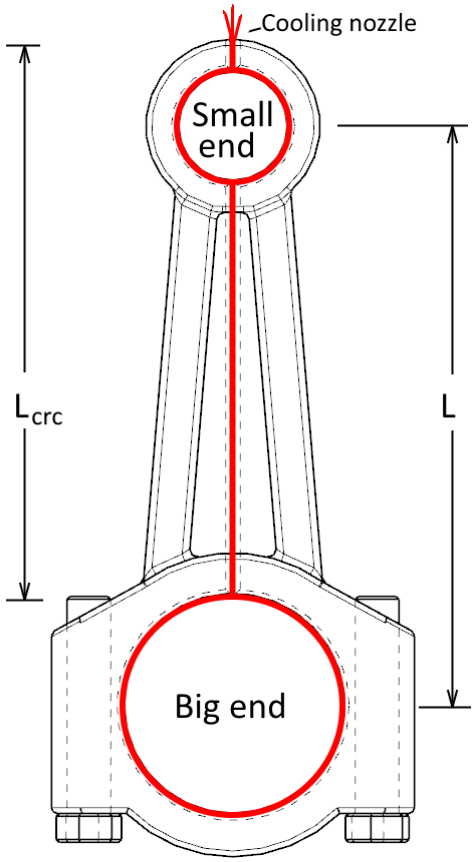

FIGURE 6.12: The connecting rod with the oil channels in red and the nozzle at the top. The rod length L is between the centres

When modeling the connecting rod some simplification is made. At the top and bottom end the oil track goes around the circumference. For simplicity, these reservoirs is modelled as an volume that is implemented with an C element calculated with **Equation 6.2**. **Figure 6.13** shows the implementation. The length of the oilchannel L_{cr} used to calculate the values in table **Table 5.1** is considered the same as the connecting rod length L, however this could be experimented with. r_{crc} is the radius of the channels in the con-rod. The number of mode representations was found by evaluating the step response of the system, and adding more elements until the results were not changing signifficantly. The same procedure was done on the crankshaft, where only one term was used in the end.

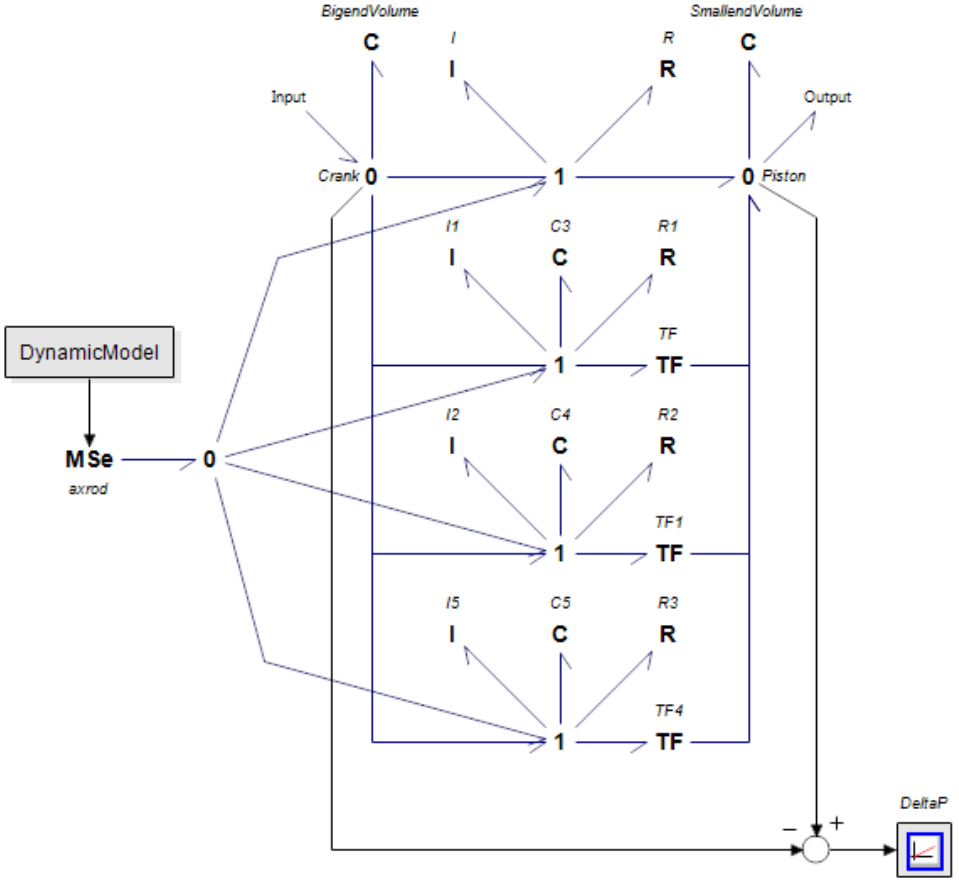

FIGURE 6.13: Connecting rod modal representation of the oil channel, pressure differential is monitored.

6.2.8 Dynamic model

The model developed in chapter **Chapter 3** is calculated with equation blocks and seen in **Figure 6.14**. It will control the connecting rod pipe with the modified set effort *MSe* element seen in **Figure 6.13**. In the final model **Figure 6.15**, the *MSe* element sets the effort to a *Zero Junction* where the effort is equal for all powerbonds. The logic block controls the bearings turning the flow on and off.

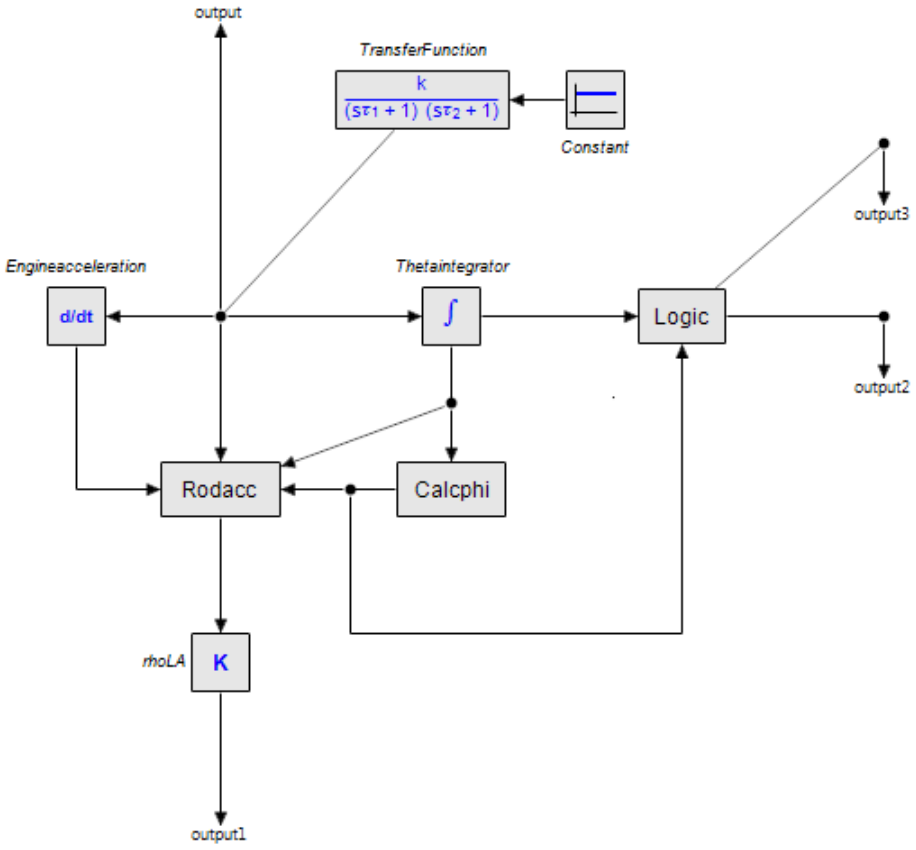

FIGURE 6.14: The dynamic model, a transfer function is used for soft starting.

6.3 Final model

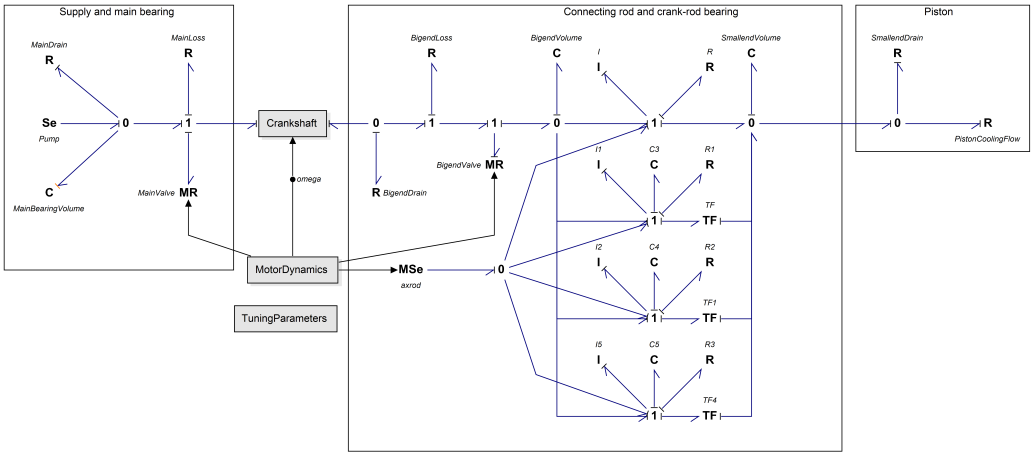

FIGURE 6.15: The complete bond-graph

The final model is seen in **Figure 6.15** and a bigger version in **Appendix C**. The crankshaft submodel contains **Figure 6.8**. Important parameters is shown in **Table 7.1**.

Chapter 7

Model testing and verification

7.1 Introduction

20-sim will develop the system equations based upon the same principle as in **Chapter 4**. Parameters that will be used is listed in **Table 7.1**. The model of the connecting-rod channels has to be solved implicitly due to stiff properties of the modal pipe-model. Backward Differentiation Formula therefore chosen. Some minor modifications also had to be done. The bearing flow loss elements was causing convergence problems during solving, simply adding a very small inertia junction to the same 1-junction as the R_{Loss} element **Figure 6.11** solved the problem.

7.1.1 Dynamic model

The dynamic model is started softly such that the solution can converge easier in the beginning. **Figure 7.1** shows how the dynamic model behaves. The con-rod acceleration ax_r is verified with the matlab plot **Figure 3.2**.

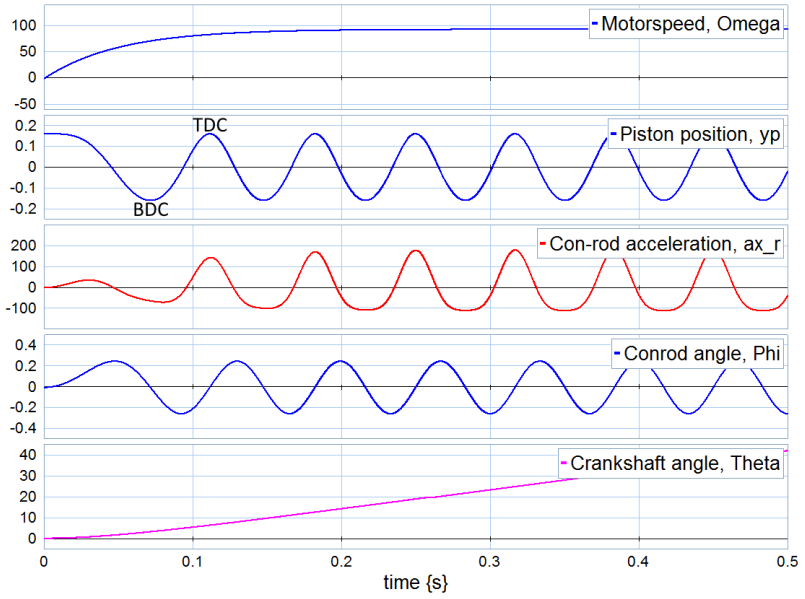

FIGURE 7.1: The values calculated by the dynamic model

Oil pump pressure	P_{set}	3 Bar *
Oil kinetic viscosity (SAE 40W 70^{o}C)	ν	$50 \cdot 10^{-5}$ Pas
Oil bulk modulus	β	$1.5 \cdot 10^{9}$ Pa
Oil acoustic velocity	a	1460 m/s
Piston cooling flow	K_d	6 l/min *
Engine speed	n	750 RPM
Connecting rod length	L	0.8 m
Connecting rod channel length	l_{crc}	0.8 m
Connecting rod channel radius	r_{crc}	5 mm *
Crankshaft stroke radius	R	0.2 m
Crankshaft channel radius	r_{csc}	10 mm *
Crankshaft channel length	l_{csc}	0.5 m
Main bearing volume	V_{main}	100 ml *
Bigend bearing volume	V_{bigend}	100 ml *
Smallend bearing volume	$V_{smallend}$	010 ml *
Main bearing flowthrough coeff	R_{mf}	$10 \cdot 10^{3}$
Big-end bearing flowthrough coeff	R_{cf}	$10 \cdot 10^{3}$
Big-end drain coefficient	R_c	$3.3 \cdot 10^{-11}$ *
Main drain coefficient	R_m	$3.3 \cdot 10^{-11}$ *
Small-end drain coefficient	R_p	$2.4 \cdot 10^{-11}$ *

TABLE 7.1: Model parameters, * parameters were assumed.

7.1.2 Verification of the connecting rod pipe model

For verifying the design of the connecting rod is to apply a static acceleration for a defined length tube. The pressure difference due to an accelerated closed oil-filled tube:

$$\Delta P = \rho a L \tag{7.1}$$

For a oil-filled tube length L = 0.8m and density ρ =800 Kg/m^3 exerted to a acceleration a of 150G, Δ P = 941760 Pa, or 9.4 Bar. Analyzing the model in **Figure 6.13**, we see that after some time ΔP converges to value.

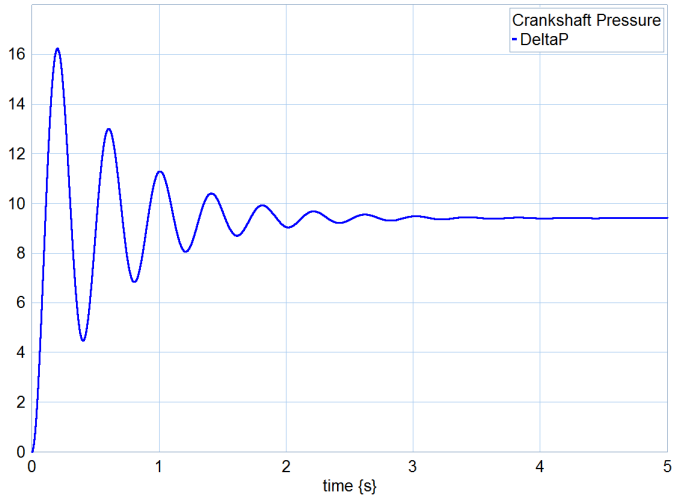

FIGURE 7.2: Testing the connecting rod pipe model with a static acceleration of 150 G

Figure D.6 and **Figure D.7** shows how the con-rod model **Figure 6.13** reacts to a impulse response. The model was isolated from the rest of the system. It shows that the pipe critical frequency is at a frequency well beyond the motion of the system, at 12.5 Hz for 750 RPM.

7.2 Comparing the model with Kang's results

The model is set up with the parameters given in **Kang [3]**, these are given in **Table 7.2**. In Kang's research, a six cylinder marine diesel engine was analyzed and the average cooling flow for each cylinder is about 6 l/min. The tracks of the bearings is assumed to go all the way around the journals, giving a constant supply throughout the cycle. Some parameters was not available and had to be approximated.

Oil pump pressure	P_{set}	7 Bar
Oil kinetic viscosity (SAE 40W 70^{o}C)	ν	$50 \cdot 10^{-5}$ Pas *
Oil bulk modulus	β	$1.5 \cdot 10^{9}$ Pa *
Oil acoustic velocity	a	1460 m/s *
Piston cooling flow	K_d	6 l/min *
Engine speed	n	600-900 RPM
Connecting rod length	L	0.64 m
Connecting rod channel length	l_{crc}	0.64 m
Connecting rod channel radius	r_{crc}	5 mm
Crankshaft stroke radius	R	0.1 m
Crankshaft journal radius	R_1	0.1 m *
Crankshaft channel radius	r_{csc}	10 mm *
Crankshaft channel length	l_{csc}	0.3 m
Main bearing volume	V_{main}	100 ml *
Bigend bearing volume	V_{bigend}	100 ml *
Smallend bearing volume	$V_{smallend}$	10 ml *
Main bearing flowthrough coeff	R_{mf}	$10 \cdot 10^{3}$
Big-end bearing flowthrough coeff	R_{cf}	$10 \cdot 10^{3}$
Big-end lubrication coefficient	R_c	$3.3 \cdot 10^{-11}$ *
Main lubrication coefficient	R_m	$3.3 \cdot 10^{-11}$ *
Small-end lubrication coefficient	R_p	$2.4 \cdot 10^{-11}$ *

TABLE 7.2: Kang model parameters. * Approximated.

Kang uses the characteristics method approach for modelling the channels in the connecting rod. Some of his results is shown in **Figure 7.3**. Q is the oil flow through the connecting rod, H_u the pressure head at the big-end and H_d the small-end pressure head.

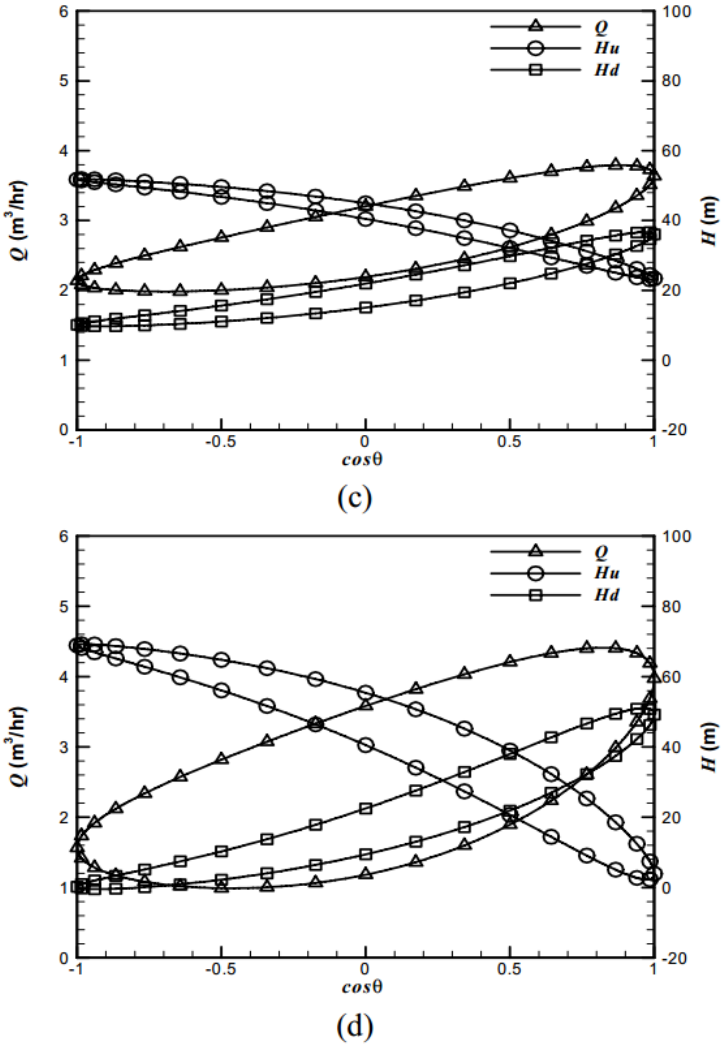

FIGURE 7.3: Plotting the flow and pressure distribution in the rod at 600 and 900 RPM, oil flow is the sum of all 6 cylinders (**Kang [3]**, Figure 5 c and d)

We see that in our plots there are similarities at both 600 and 900 RPM. It can be seen that the graphs has a lower phase shift, giving a less circular shape. This could be that the inertia, or friction loss model is different. Comparing to Kang the lines are: [Q: Blue line], [Hu: Pink line], [Hd: Green line]

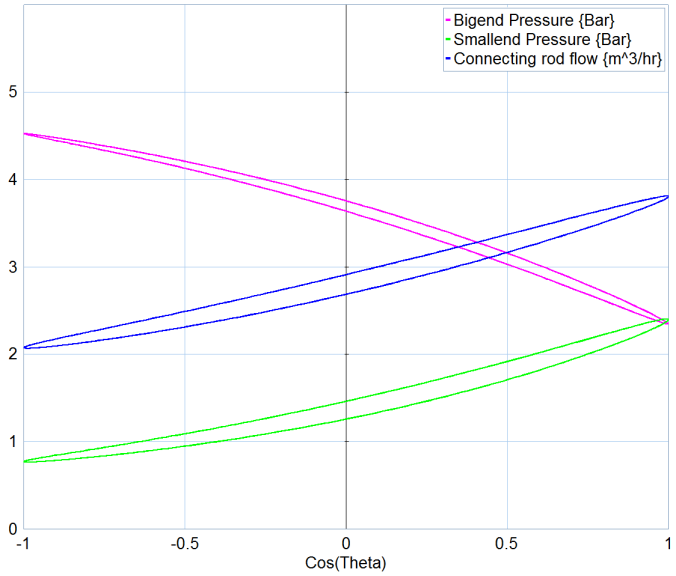

FIGURE 7.4: 600 RPM. Note that the y-axis is shared

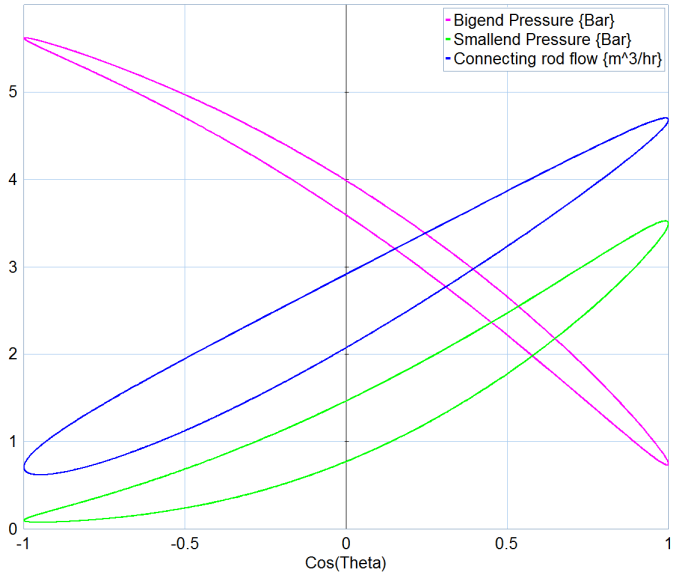

FIGURE 7.5: 900 RPM. Shared y-axis

7.3 Summary

The model was tested and the result showed that the model responds intuitively. Adjusting the parameters, we can adapt the model for a variety of designs.

Chapter 8

Results

8.1 Dry run

An analysis was done to see how the pressure at the big and small end is affected in the connecting rod. The cooling nozzle flow was set to zero, as well as all the bearing lubrication flows. Setting the oil pump pressure to zero, we see the pressure in the small-end is almost proportional to the acceleration force. The big-end pressure is shifted up a little, this is from the pressure amplification of the crankshaft.

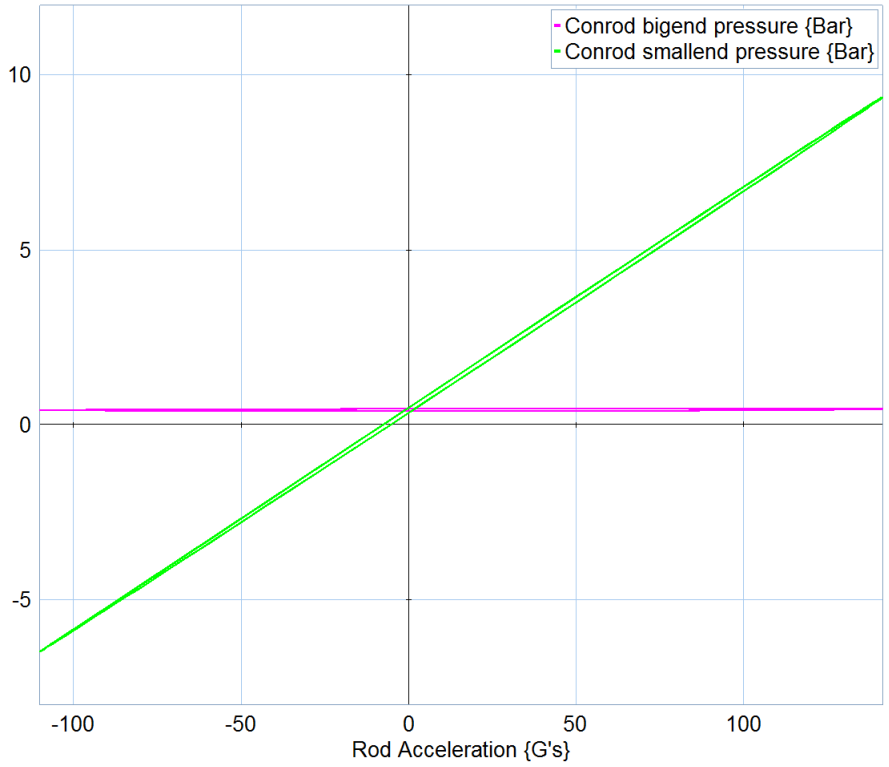

FIGURE 8.1: Dry run of the system. 750 RPM, $P_{set} = 0$ Bar. No bearing drain or cooling

8.1.1 Adding lubrication drain and pump pressure

We also apply the oil drained by the bearings, red and black line in **Figure 8.2**. The oil then starts flowing in the connecting rod and the result is that the small-end pressure becomes phase shifted due to the inertia of the fluid. 6.6 bar from the oilpump was needed to attain a positive pressure in the small-end throughout the cycle. This is rather high.

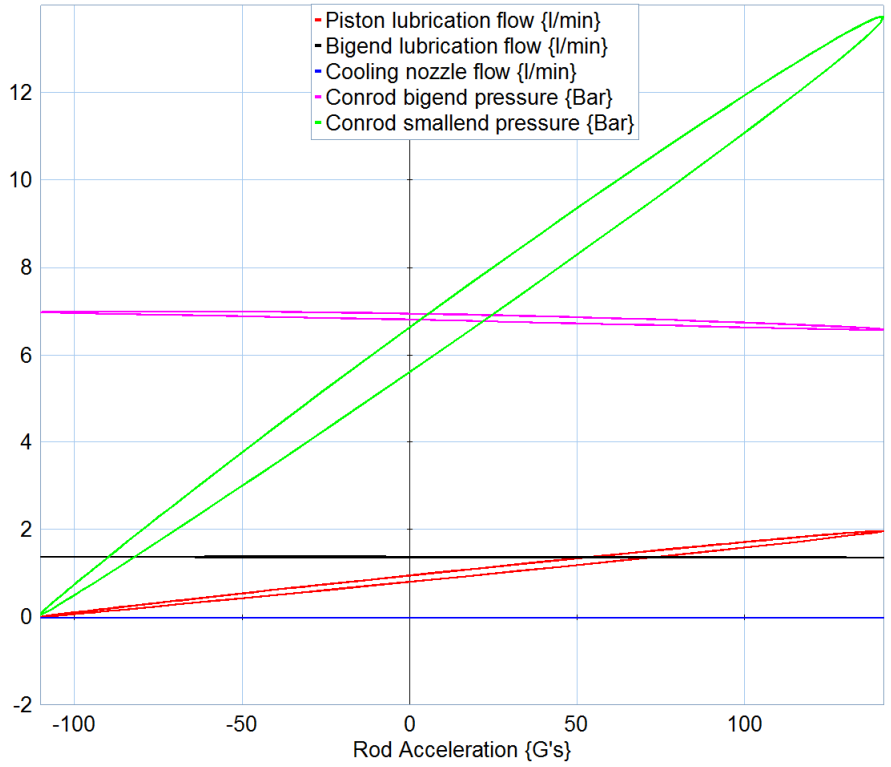

FIGURE 8.2: The graphs become more circular due to inertia forces. 750 RPM, P_{set} = 6.6 Bar. Bearing drain is active on all bearings

8.1.2 Adding the cooling nozzle flow

Finally we add an average cooling of 5 litre per minute by adjusting K_d, blue line in **Figure 8.3**. The flow in the con-rod increased and the inertia forces puts an extra phase shift in the small-end pressure. The big and small-end pressure was affected significantly due to flow-losses.

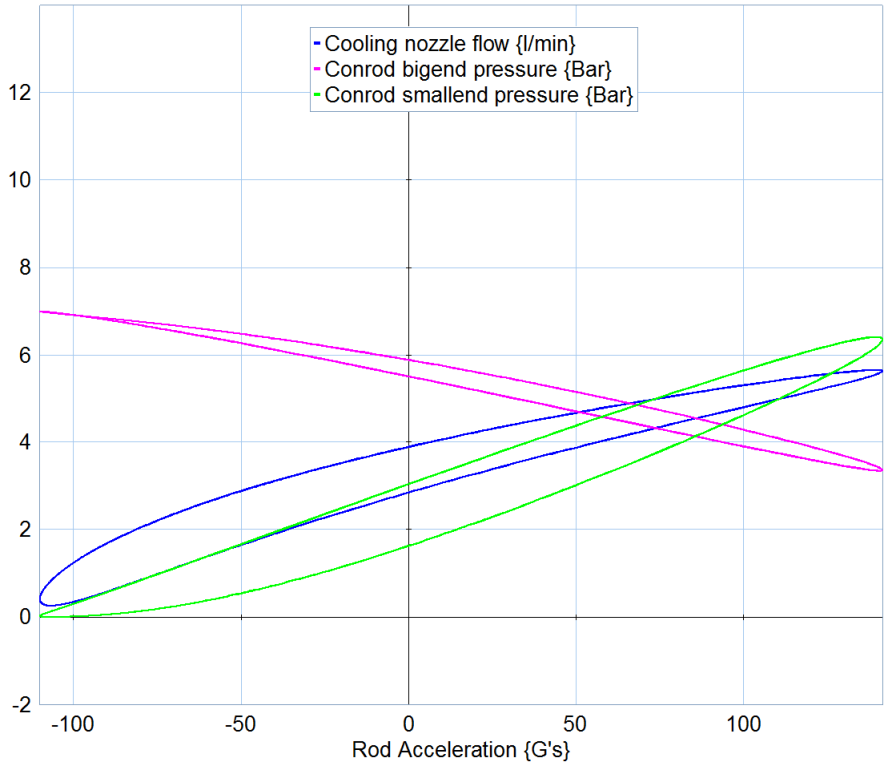

FIGURE 8.3: Adding 5 l/min of cooling flow. The pressures was lowered globally due to flow losses.

8.1.3 Using a smaller channel in the crankshaft

To test the arguments in **Section 2.2**, we lowered the crankshaft channel diameter from 10 mm to 5mm. This restricted the flow to the connecting rod and the nozzle flow was negative at BDC. It would mean that the nozzle might be sucking air, something the model does not take account for. If the nozzle sucked in air the oil would return very fast when the piston approaches the TDC region. The reason is the low viscosity of the air. When all the air has escaped, the oil hits the nozzle with a high velocity and the crashing force can break it or cause eroding cavitation. The result shows that the delivery through the crankshaft is important.

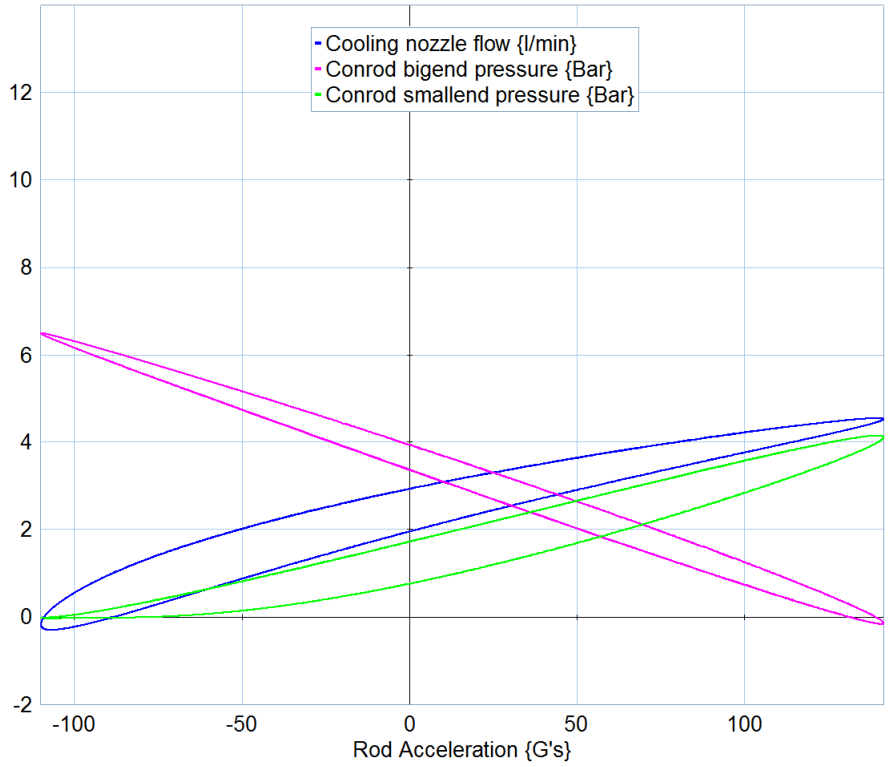

FIGURE 8.4: Crankshaft chanel diameter = 5mm, reducing the flow to the con-rod and lowering the system pressure

8.2 Using half-closed bearing tracks at the rod

After analyzing the model, it is clear that the pressure distribution is very much affected by the motions in the system. The result is that for the higher speed, the higher the oil supply pressure needs to be. Otherwise, the pressure at the small end will be sub zero at BDC, and the cooling nozzle will suck air into the con-rod. If the designer of the engine use bearing tracks that closes the flow when the piston is in the BDC region he could use a lower oil supply pressure. Using a lower pressure means that less pumping energy is wasted and the engine will use less fuel. The crankshaft would be modified to have only one input hole.

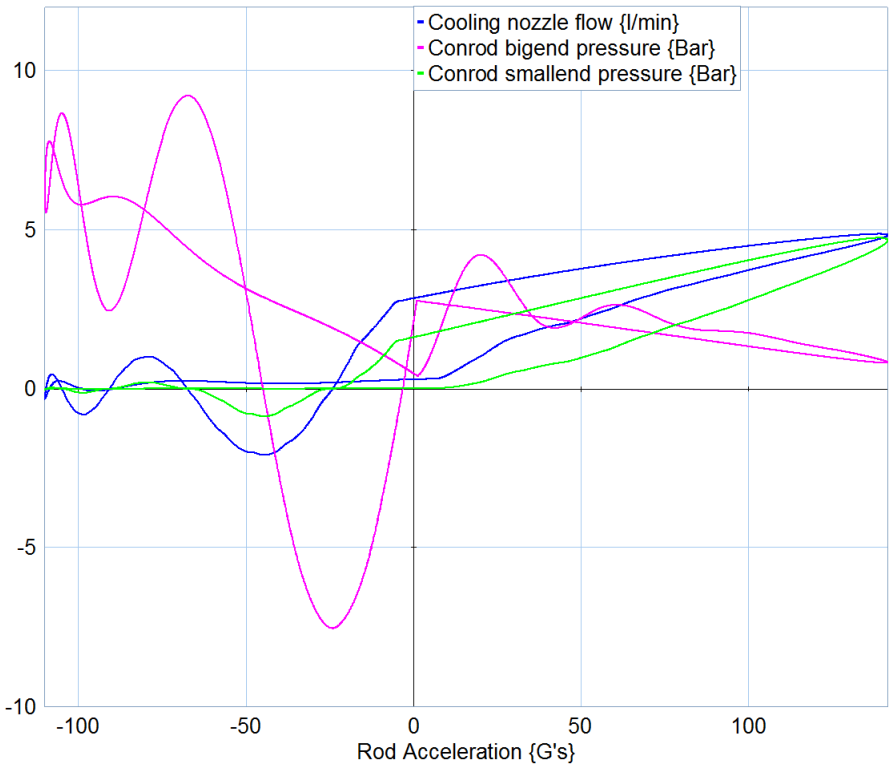

FIGURE 8.5: $P_{set} = 3bar$. The flow is stopped in the BDC region. Transients occur due to the "water hammer effect". However the oil can not exit the con-rod at the big-end

As seen in figure 8.5 blocking the flow around BDC could be an solution to stop reverse flow. However the pressure variations due to the "water hammer effect" can initiate cavitation which that erode metal. According to **Kang [3]** the cavitation initiates at the big-end of the con-rod. Looking at the pressure variations at the big end the statement seems valid. Note that the equations used for modelling the con-rod pipe is not valid if cavitation or column separation occurs. Something that would be likely in this case.

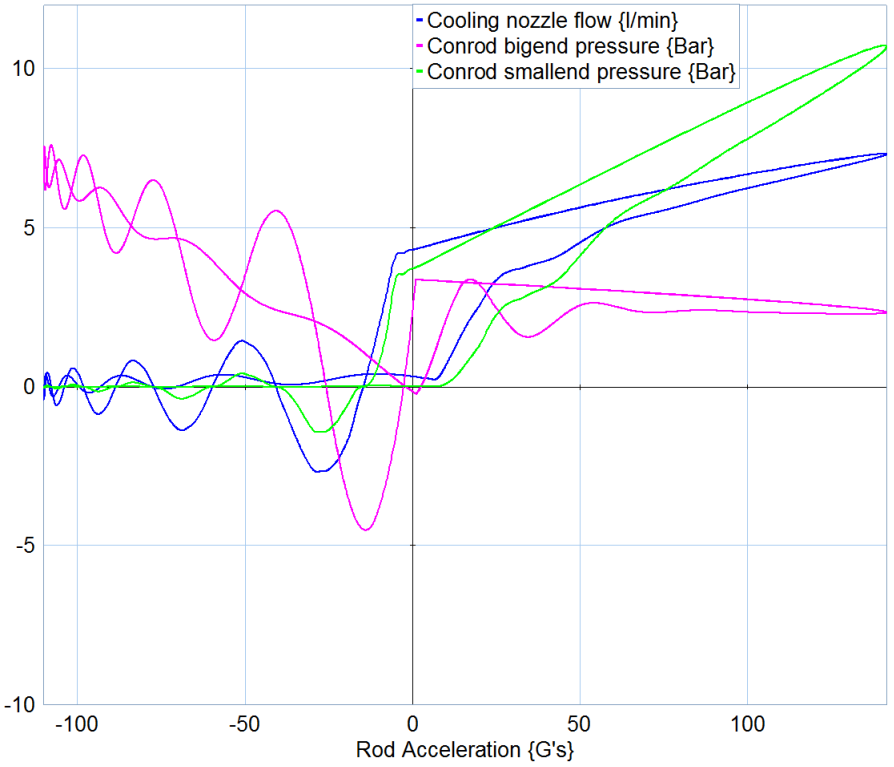

FIGURE 8.6: Increasing the con-rod tube, $r_{crc} = 10mm$

Experimenting with the size of the tube in the connecting rod, the flow velocity and inertia forces was reduced. The result was higher frequency but lower amplitude pressure waves **Figure 8.6**. Also increasing the big-end bulk-volume to 400ml decreased the pressure spikes, **Figure 8.7**. The small-end volume also had an effect if it was over half of the value of the big end volume.

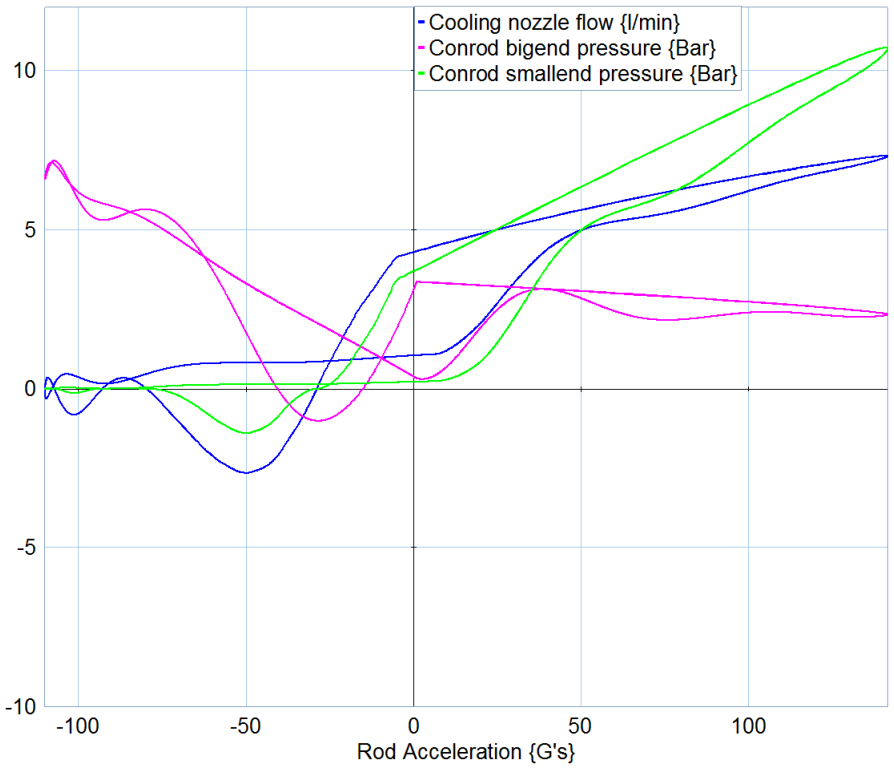

FIGURE 8.7: $V_{bigend} = 400\text{ml}$. $r_{crc} = 10mm$. The negative pressure valley in the big end was reduced

Other ways to control the flow was done by having only half track only at the main bearing. The main bearing closes in the region $[\frac{\pi}{2} < \theta < \frac{3\pi}{2}]$ instead of $[\frac{\pi}{2} < \theta + \alpha < \frac{3\pi}{2}]$ for the con-rod bearing **Figure 8.8**. The results showed lower amplitude pressure spikes, but the oil in the connecting rod exits through the big-end bearing. The cooling nozzle would then suck air.

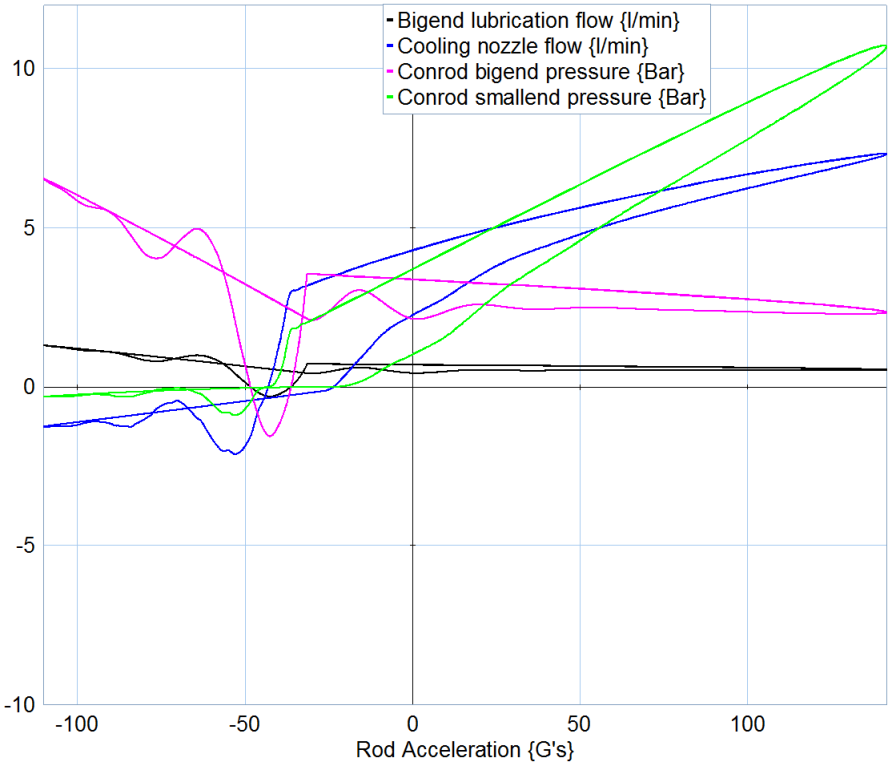

FIGURE 8.8: Using half-track bearings only at the main bearing the spikes lower, but the big-end bearing is draining oil. $r_{crc} = 10mm$

Choosing bearing shells that gradually switches the flow by having the track width gradually decrease in depth seemed to be the best solution, **Figure 8.9**. This design had much headroom in tuning other parameters without causing much problems. The reason was that the cause of the "water hamer effect" was reduced in the first place.

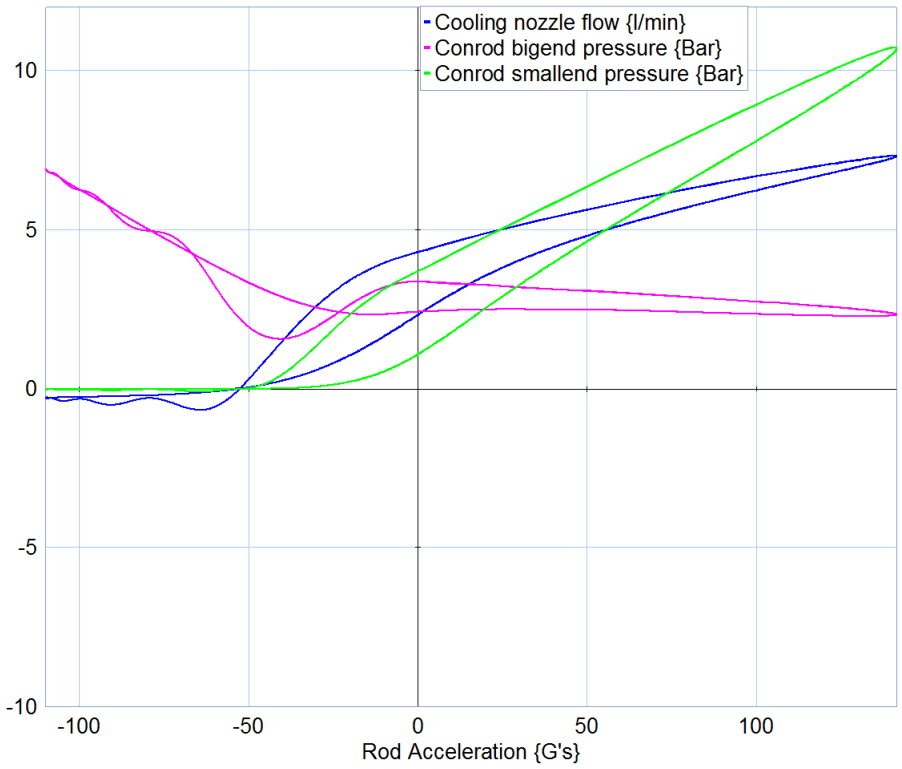

FIGURE 8.9: Bearings that switch the flow gradually. $R_{crc} = 10mm$

8.2.1 Reynolds number

To verify if the flow can be considered laminar, the Reynolds number is evaluated and should be under should be under 10^4. **White [6]**. Plots including the Reynolds number can be seen in **Appendix D**.

$$Re = \frac{DV\rho}{\nu} \tag{8.1}$$

Where

- D is the diameter of the tube - V is the velocity in the tube

Chapter 9

Conclusion and Further work recommandations

9.1 Conclusion

As seen, the oil in the connecting rod is highly affected by the reciprocating motion of the part. For the fully open system it was concluded that the pressure had to be very high to ensure a positive pressure during the cycle. Secondly it was shown that a low flow loss through the crankshaft was important. Using bearing tracks that controlled the flow would introduce large pressure waves especially at the big-end. Adjusting the parameters and bearing-track characteristics gave great results in controlling these waves to a extent where they most likely would not cause cavitation. The best option was clearly to control the flow through the bearings gradually.

9.1.1 System behaviour comment

The model responded very predictable to the changes made, also it had have some headroom within a good design where a set of parameters could be chosen without causing much problems. The bode diagrams in **Figure D.6** and **Figure D.7** tells us that the critical frequency is very high, about 500 Hz compared to the 12.5 Hz cycle time at 750 RPM. It was seen in the plots that the phase-shift was never severe.

9.1.2 Other ways of controlling the transients

For an engine running at a range of speeds, it is important to control the transient at a wider range of frequencies. Smooth bearing-track characteristics might not be smooth enough at higher RPM. As suggested by **Kang [3]**, a orifice can be installed to control the transients. Other solutions could be to install a one-way check valve **Figure D.8**, or an porous section of sintered balls in the channels. The Ergun equation **Darby [8]** calculates the flow-friction through sintered materials. It has a linear term and a quadratic term. Progressive friction could be useful for restricting the transients but not the actual flow for a variety of engine speeds.

$$e_f = 1.75\frac{V_s^2}{d}\Big(\frac{1-\epsilon}{\epsilon^3}\Big)L + 180\frac{V_s\mu(1-\epsilon)^2L}{d^2\epsilon^3\rho} \tag{9.1}$$

Where:

- e_f is the energy dissipated per unit mass of fluid
- d is the particle diameter
- ϵ is the porosity or void fraction
- V is the velocity [L/s]
- ν is the kinematic viscosity
- ρ is the density of the fluid transported
- L is the transport length

9.2 Further work recommandations

The most important part in this analysis is clearly the connecting rod. The supply through the crankshaft had an importance, but as long as it could deliver an acceptable amount of oil it did not cause much problems. More focus on the oil transport through connecting-rod alone should be done. A list is given:

1. The model should be verified by experiments.
2. The dissipating friction in the oil channels should be modeled with laminar-viscous models.
3. The channels in the connecting rod could be modeled with more accurate to the actual design.
4. The bearing loss and drain coefficients should be verified as a CFD analysis was not acheived.
5. Analyzing an actual engine design would be beneficial, bearing drain and cooling flow-rate are important parameters.

Appendix A

Bond graph extra

The table is gathered from **Pedersen-Engja [5]**. A compendium about bond graph modelling.

Bond graph element	**Constitutive relations**
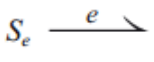	$e = e(t)$
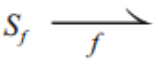	$f = f(t)$
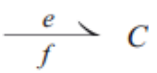	General : $q = \Phi_C(e)$ Linear : $q = Ce$
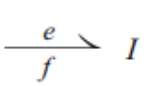	General : $p = \Phi_I(f)$ Linear : $p = If$
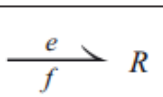	General : $e = \Phi_R(f)$ Linear : $e = Rf$
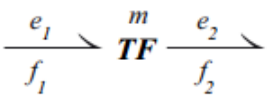	$e_1 = me_2$ $mf_1 = f_2$
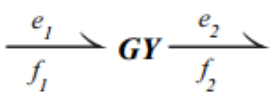	$e_1 = f_2 r$ $f_1 r = e_2$
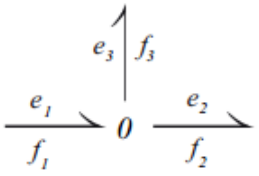	$e_1 = e_2 = e_3$ $f_1 - f_2 - f_3 = 0$
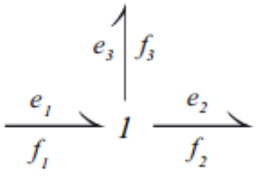	$f_1 = f_2 = f_3$ $e_1 - e_2 - e_3 = 0$

Table 2.2 : Basic bond graph elements

Appendix B

Graphic CAD model

This illustrative CAD model of the crank system was made in Siemens UGS NX by the author.

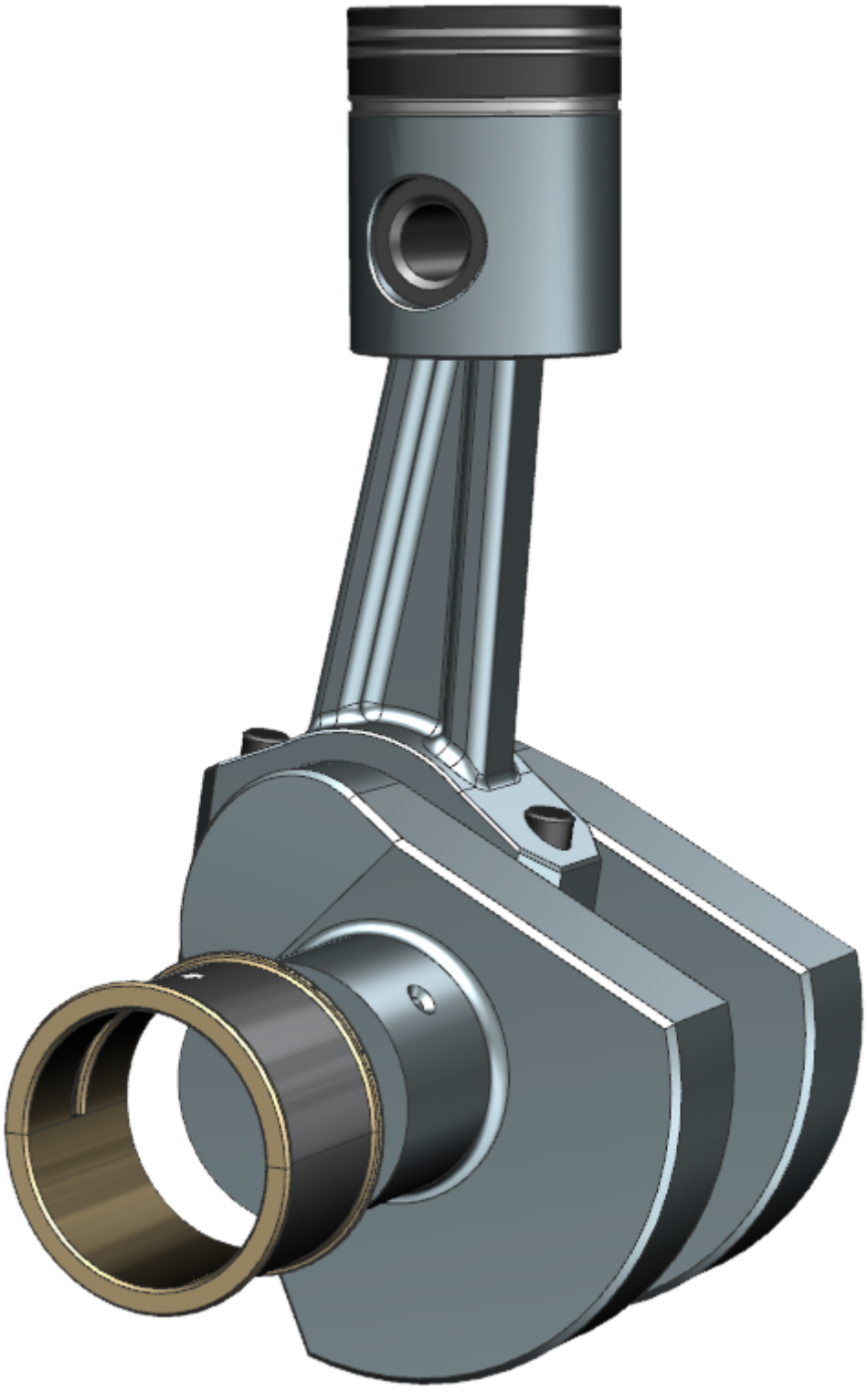

FIGURE B.1: Complete assembly, the bearing shells are pulled out to illustrate the tracks and the inlet to the channel in the crankshaft.

Appendix C

System models

This appendix includes bigger versions of **Figure 6.1** and **Figure 6.15** from chapter 6.

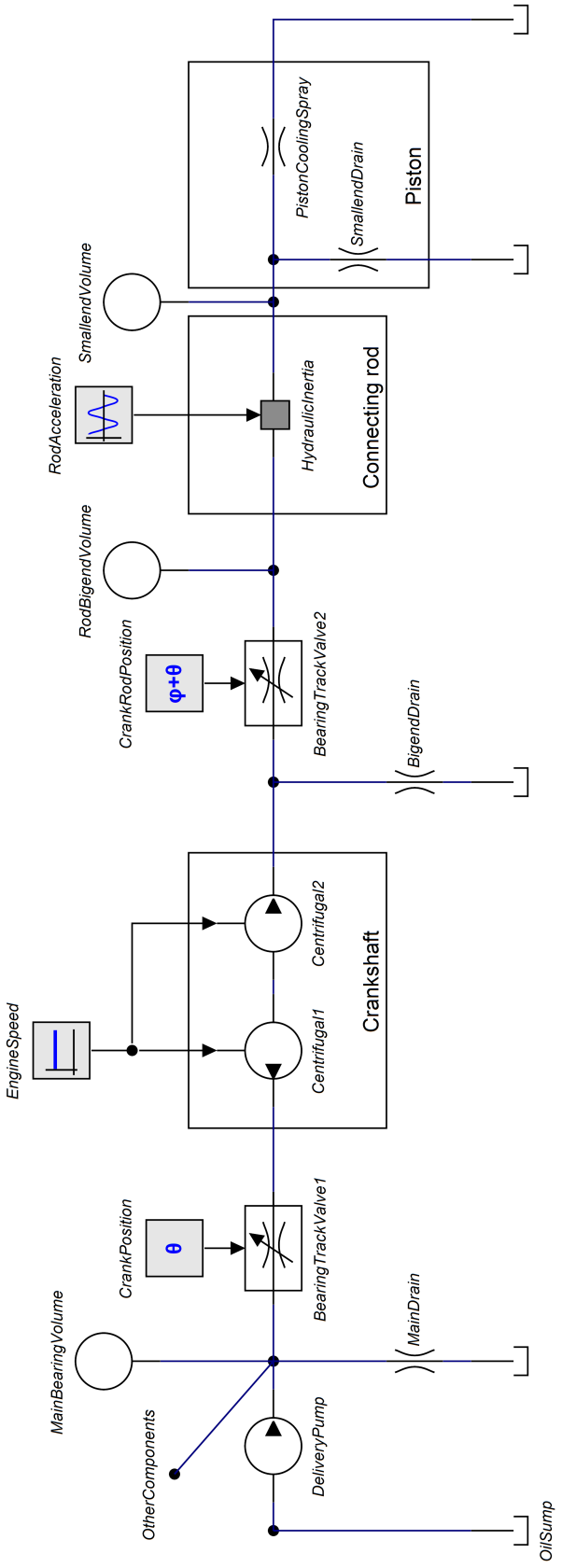

FIGURE C.1: The hydraulic diagram

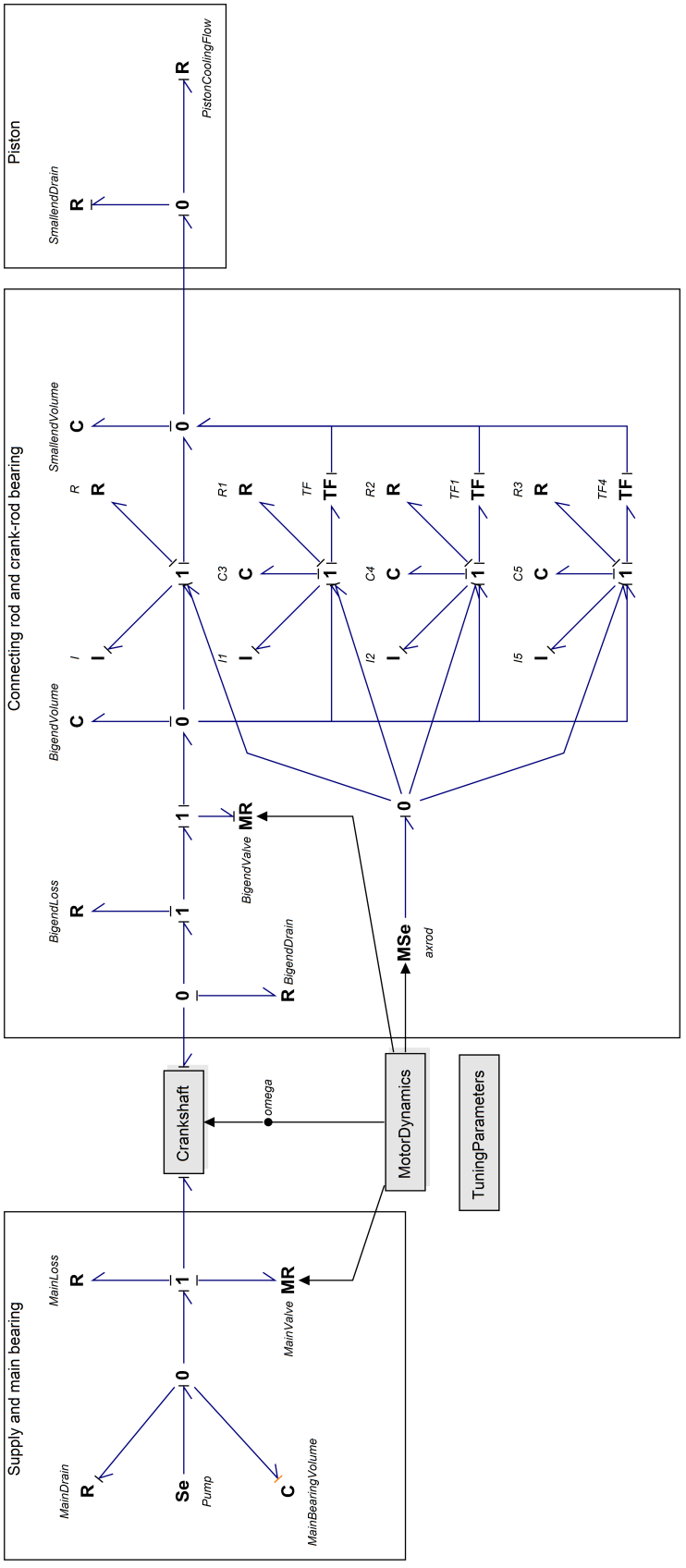

FIGURE C.2: The complete bond-graph model

Appendix D

Extra analyses

First two plots show flow and pressure in a system that is fully open. The bearing tracks do not control the lubrication-flow.

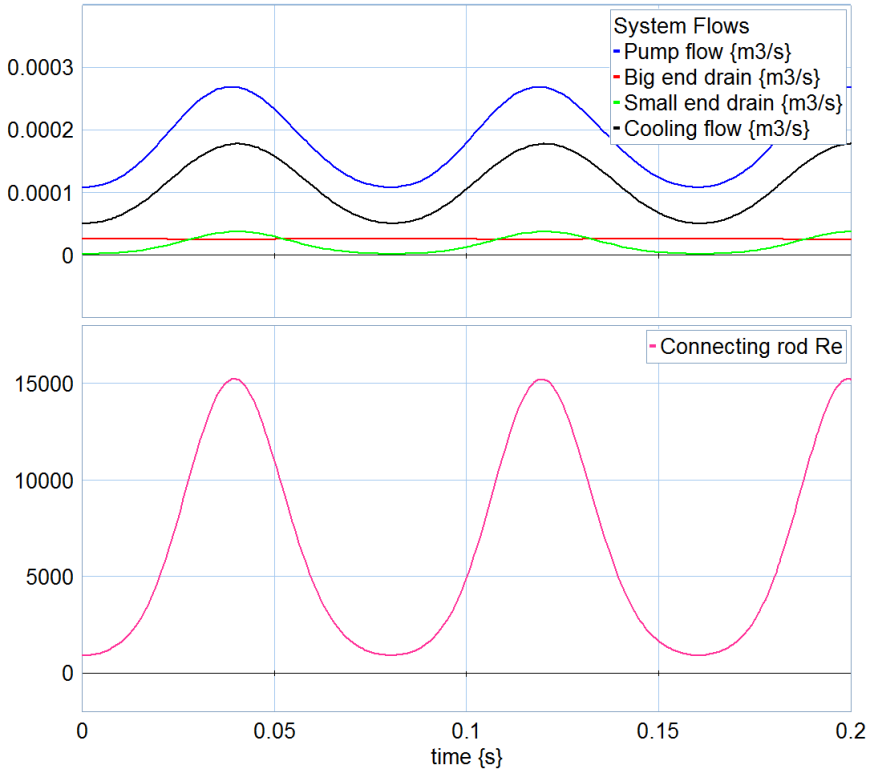

FIGURE D.1: $r_{crc} = 10$ mm. Comparing the flow-drain in the open system. The Re number indicates that turbulent flow is likely.

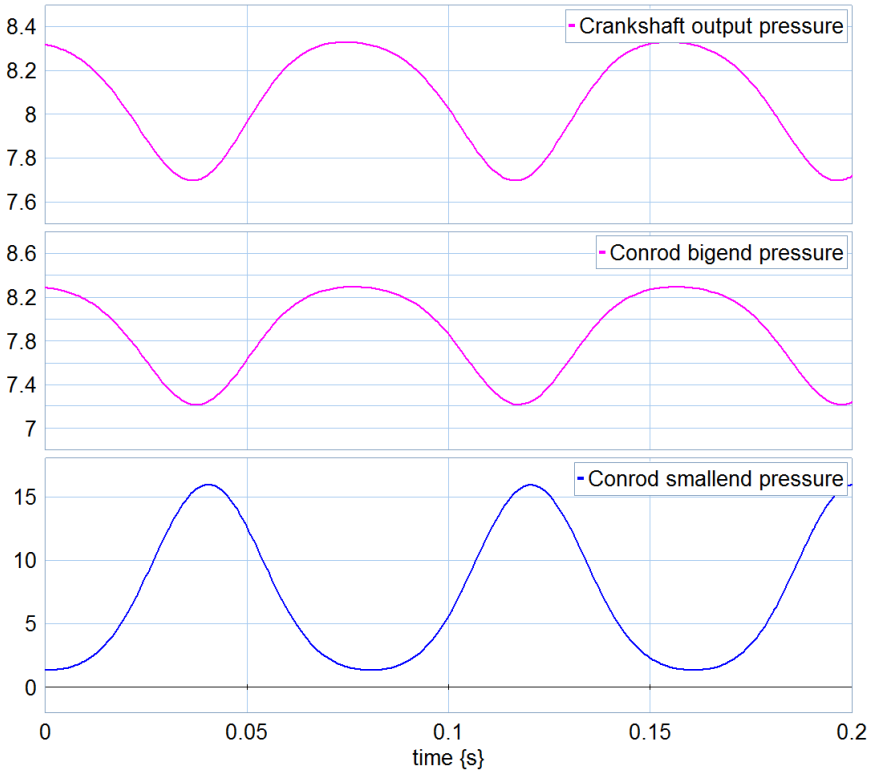

FIGURE D.2: $r_{crc} = 10$ mm. Pressure in the open system.

Two plots for a system that is softly controlled by the bearing tracks:

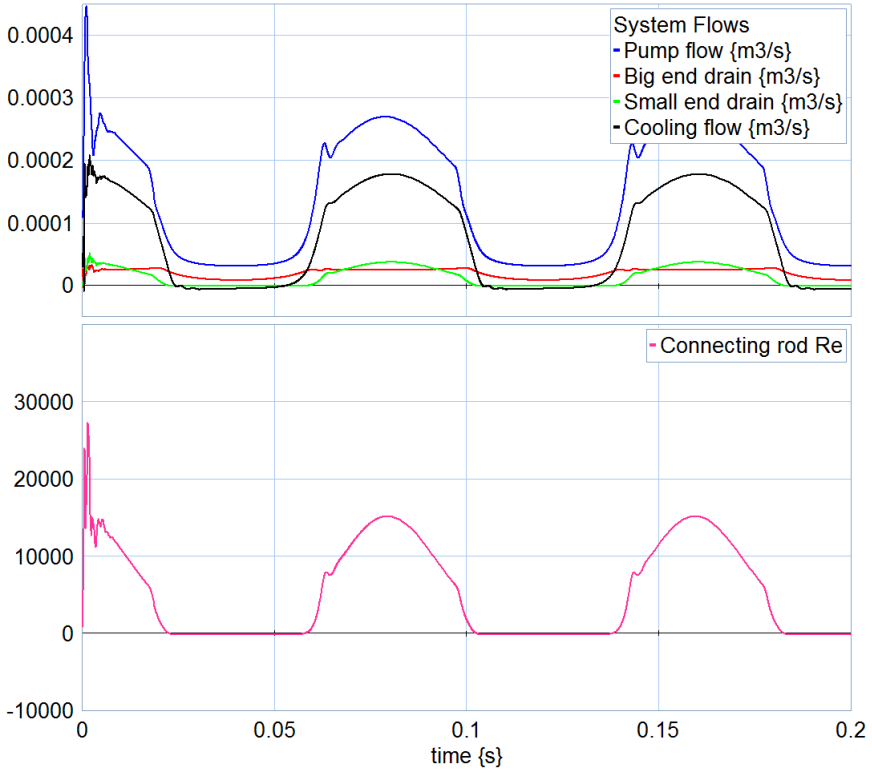

FIGURE D.3: $r_{crc} = 10$ mm. Comparing the flow-drain in the flow controlled system. The Re number indicates that turbulent flow is likely.

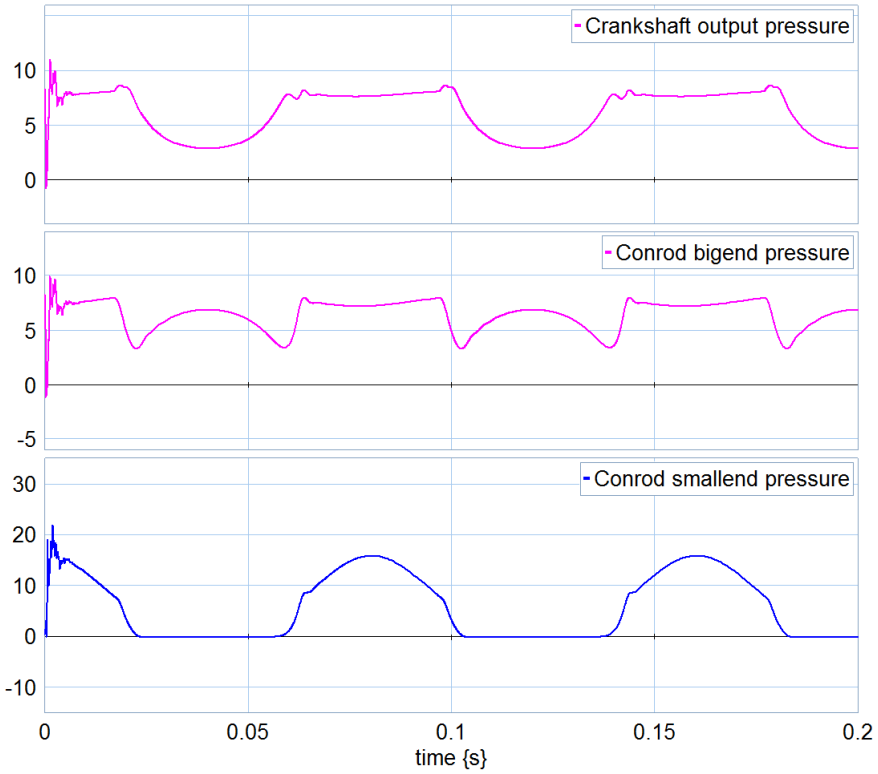

FIGURE D.4: $r_{crc} = 10$ mm. Pressure in the flow controlled system.

A run from 0 to 750 RPM withsmooth bearing valves showed no tendency of critical frequencies.

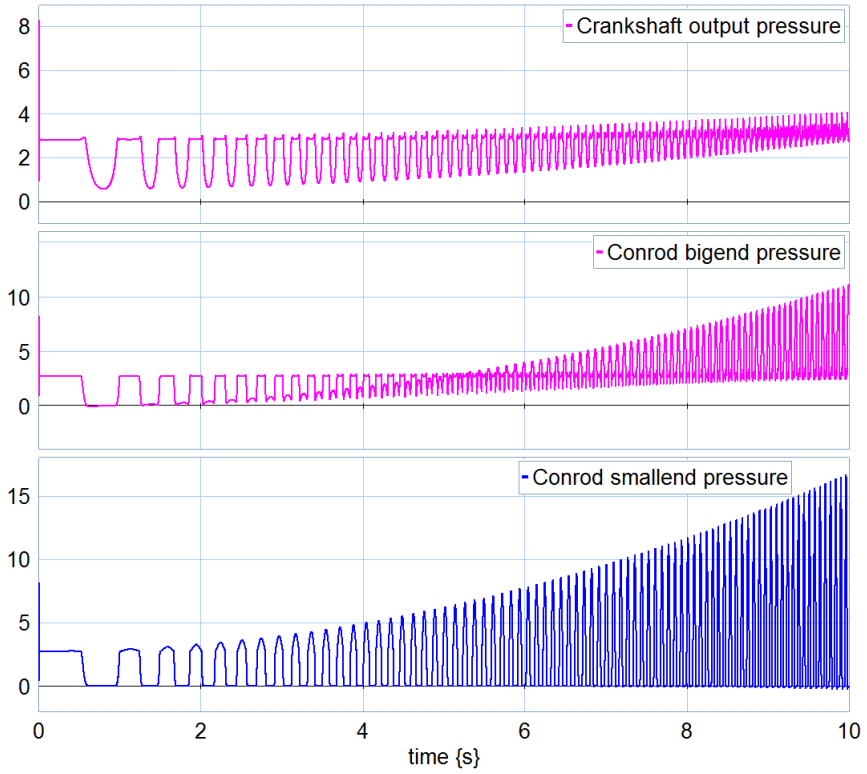

FIGURE D.5: Pressure at the small end from 0 to 750 RPM for the flow controlled system. $r_{crc} = 10\text{mm}$ $p_{set} = 3$ Bar

Some impulse response of model in **Figure 6.13**. The frequency response is dependent on the tube length. Higher values of the small and big-end volumes give lower critical frequency.

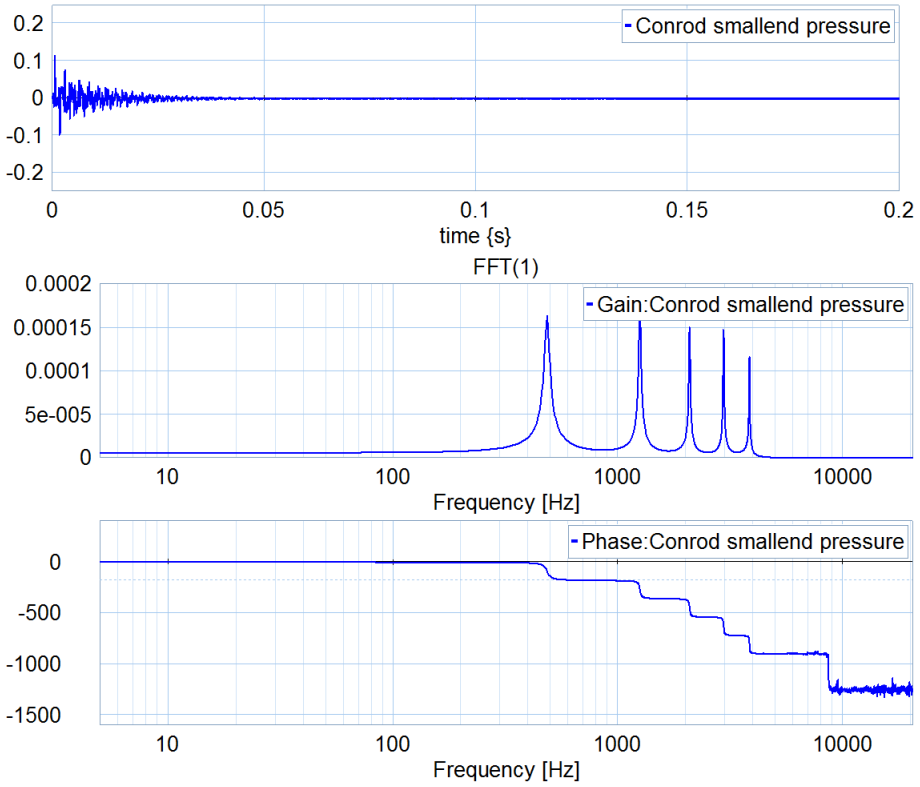

FIGURE D.6: $r_{crc} = 5$mm. Step response FFT analysis of the smallend

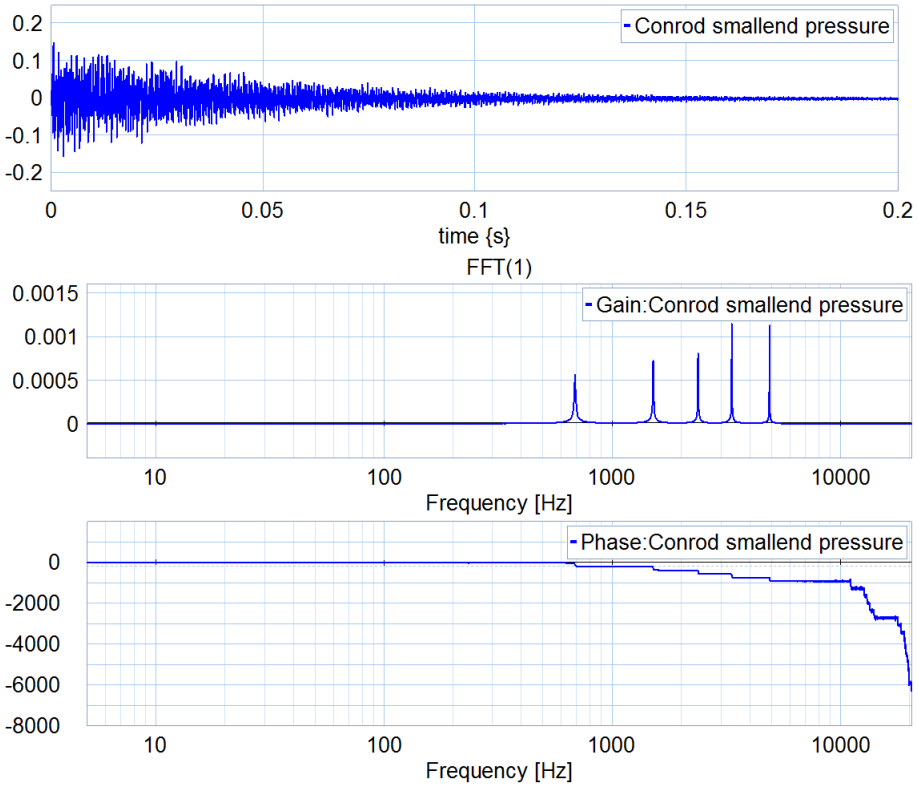

FIGURE D.7: $r_{crc} = 10$mm. Step response FFT analysis of the smallend

The model was tested with an check-valve at the big-end that only allowed flow towards the piston **Figure D.8**. Bearing tracks was open during the whole cycle. The result showed very smooth system, and could be a solution to having a low pressure delivery pump.

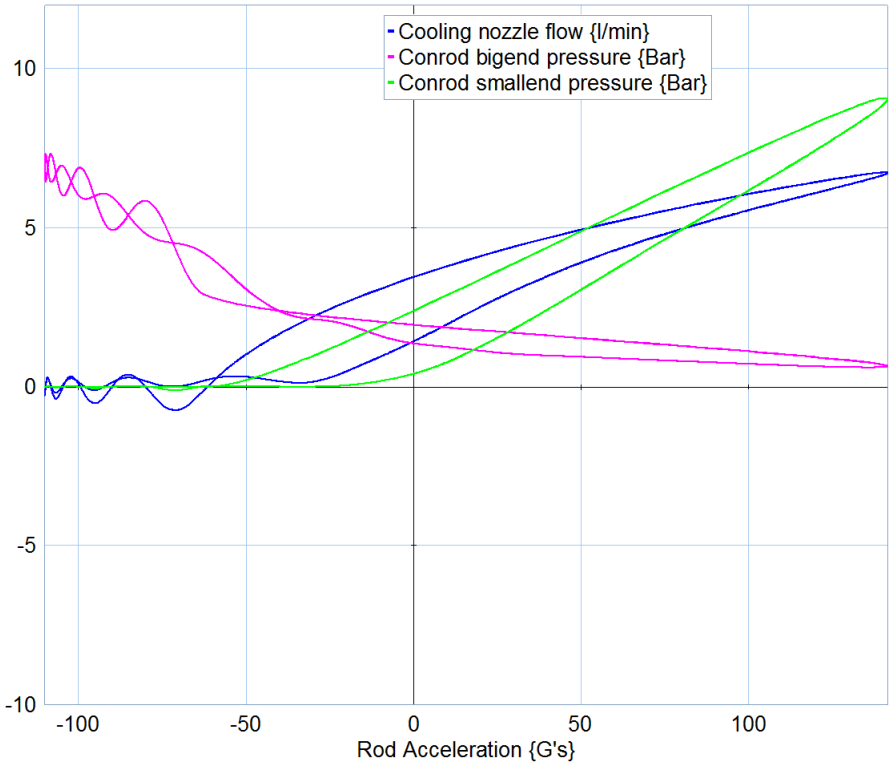

FIGURE D.8: Check valve allows flow only towards the piston

Appendix E

Various code

```
parameters
   real global rho;
   real global R;
   real global rj;
variables
   real flow;
equations
   p.e = 0.5 * rho * effort^2 * (R^2 - rj^2);
   flow = p.f;
```

FIGURE E.1: Code for pressure amplification of crankshaft.

```
parameters
   real global K_d;
   real global A_d;
   real global rho;
equations
   p.f = K_d * A_d * sqrt( 2 * abs(p.e) / rho) * sign(p.e);
```

FIGURE E.2: The code for the nozzle R element

```
parameters
   real global R_mf;
equations
   p.e = R_mf * p.f^2 * sign(p.f);
```

FIGURE E.3: The code for the flow-through of the main bearing in this case

```
//This controls the bearing valves
equations
//Mainbearing
if thetap < pi/2 then
mainbearing = 1;
end;

if thetap > pi/2 then
mainbearing = 1e12;
end;

if thetap > 3*pi/2 then
mainbearing = 1;
end;

//Crankbearing
if thetap+phi < pi/2 then
crankbearing = 1;
end;

if thetap+phi > pi/2 then
crankbearing = 1e12;
end;

if thetap+phi > 3*pi/2 then
crankbearing = 1;
end;
```

FIGURE E.4: If statements control the bearing valve function

Bibliography

[1] Eilif Pedersen

Lumped Parameter Models for Unsteady Flow Calculations Using Normal Modes and Bond Graphs

ASME - 1999.

[2] M. Lebrun

Normal Modes in Hydraulic Lines

Laboratore d'Automatique - Universite Claude Bernard Lyon - 1984

[3] Shin-Hyoung Kang, Jeon-Gu Kim, Kuyung-Nam Chung

Prediction of transient lubricating oil flows within the connecting-rod of a diesel engine

Seoul National University, Department of Mechanical Engineering - August 2010

[4] S.M. Chun

Network analysis of an engine lubrication system

Elsevier - December 2003

[5] E. Pedersen - H. Engja

Mathematical Modelling and Simulation of Physical Systems

Norwegian University of Science and Technology, Department of Marine Technology - 2010.

[6] Frank M. White

Fluid Mechanics, 7.th edition

McGraw-Hill - February 2010

[7] E. Benjamin Wylie
Fluid transients
McGraw-Hill - 1978

[8] Ron Darby
Chemical Engineering Fluid Mechanics 2.edition
Marcel Dekker - 2001